

# CHEMICAL WEATHERING, ATMOSPHERIC CO<sub>2</sub>, AND CLIMATE

---

Lee R. Kump, Susan L. Brantley, and Michael A. Arthur

*Department of Geosciences and Earth System Science Center, The Pennsylvania State University, 302 Deike Building, University Park, Pennsylvania 16802; e-mail: lkump@psu.edu*

**Key Words** chemical weathering, carbon cycle, climate change, Earth history, modeling

■ **Abstract** There has been considerable controversy concerning the role of chemical weathering in the regulation of the atmospheric partial pressure of carbon dioxide, and thus the strength of the greenhouse effect and global climate. Arguments center on the sensitivity of chemical weathering to climatic factors, especially temperature. Laboratory studies reveal a strong dependence of mineral dissolution on temperature, but the expression of this dependence in the field is often obscured by other environmental factors that co-vary with temperature. In the field, the clearest correlation is between chemical erosion rates and runoff, indicating an important dependence on the intensity of the hydrological cycle. Numerical models and interpretation of the geologic record reveal that chemical weathering has played a substantial role in both maintaining climatic stability over the eons as well as driving climatic swings in response to tectonic and paleogeographic factors.

## INTRODUCTION

The intriguing message from Quaternary geologic, isotopic, and glaciological records is that the Earth's climate system may be extremely sensitive to perturbation, especially near thresholds of changes in state between glacial and interglacial conditions. In contrast, the longer-term ( $10^8$ – $10^9$ -year) perspective reveals a climate system that is resilient in the face of external influence. In other words, most of the processes affecting climate on century to multi-millennial time scales are components of positive feedbacks, whereas those that are significant on long time scales tend to create negative feedbacks. Subtle changes within the system can be sensed and amplified through positive feedback, so that the stabilizing (negative) feedbacks can act to damp the ultimate response (e.g. Kump 1996). This enhanced sensitivity on short time scales and diminished sensitivity on long time scales is a characteristic of a stable system.

Here we focus on the long-term feedbacks so that we may address the ultimate question of whether CO<sub>2</sub> is the stabilizing climate influence over geologic time.

There are clear indications that this, in fact, is the case. Consider Earth's response to increasing solar luminosity over its 4.6 billion year history. Had the atmospheric composition of the early Earth been similar to today's, surface water on Earth would have been completely frozen prior to about 2 Ga (Sagan & Mullen 1972, Kasting 1993). Abundant geologic evidence for a vigorous Precambrian hydrologic cycle and a productive marine biota precludes this possibility, and instead leads to the prevailing theory that the atmosphere had much higher concentrations of greenhouse gases ( $\text{CO}_2$  and  $\text{CH}_4$ ) than it has now. The corollary of this solution of the Faint Sun Paradox is that some mechanism must have regulated the drawdown of these gases to prevent permanent global glaciation or extreme warmth. For example, an atmospheric  $\text{CO}_2$  partial pressure ( $p\text{CO}_2$ ) of 1,000 times the present atmospheric level (1000X PAL) would have been required to compensate for a sun 70% as luminous as today's at 4.6 Ga (Kasting 1993). Had the  $\text{CO}_2$  level fallen too rapidly, Earth might have become locked into an inescapable Snowball Earth state, and the presence of life on Earth's surface would have become impossible (Caldeira & Kasting 1992). Had that  $\text{CO}_2$  remained in the atmosphere, the global average temperature today would be at least  $45^\circ\text{C}$ , instead of its present value of  $15^\circ\text{C}$  (JF Kasting, pers. comm.). Organisms that thrive under such conditions are the thermophilic bacteria; most other groups would have been severely stressed by such warmth, and might not have persisted on Earth.

This regulation mechanism has not been perfect, and Earth has oscillated between greenhouse and icehouse states (Fischer 1982, Frakes et al 1992). These  $\sim 10^8$ -year fluctuations were most likely the result of plate-tectonic forces, which are generally considered to be external to the climate system. For example, greenhouse intervals such as the mid-Cretaceous tend to coincide with times of elevated global volcanism (Fischer 1982). As a major source of  $\text{CO}_2$  to the ocean-atmosphere system on geologic timescales, this volcanic activity would have caused an enrichment in the  $\text{CO}_2$  content of the atmosphere and a strengthening of the greenhouse effect.

On geologic time scales, the amount of  $\text{CO}_2$  in the atmosphere is determined by processes such as organic-carbon and carbonate-carbon sedimentation and burial, carbonate, organic carbon, and silicate weathering on land, and volcanic and metamorphic release of  $\text{CO}_2$  (Garrels et al 1975, Figure 1; details discussed later in this article). Many of these processes are sensitive to the state of the surface environment, including its temperature and the intensity of the hydrologic cycle. These environmental variables, in turn, are sensitive to atmospheric  $p\text{CO}_2$  through the greenhouse effect. Thus, it is reasonable to assume that there are negative feedback mechanisms at work over geologic time that stabilize atmospheric  $p\text{CO}_2$  and climate. From a modeler's perspective, if one can determine the functional dependence of these processes on atmospheric  $p\text{CO}_2$  (at least to first order), then one can estimate changes in atmospheric  $p\text{CO}_2$  that have occurred in the past as the result of changes in the rates of these processes (e.g. Walker et al 1981, Berner et al 1983). The processes that may be sensitive to atmospheric

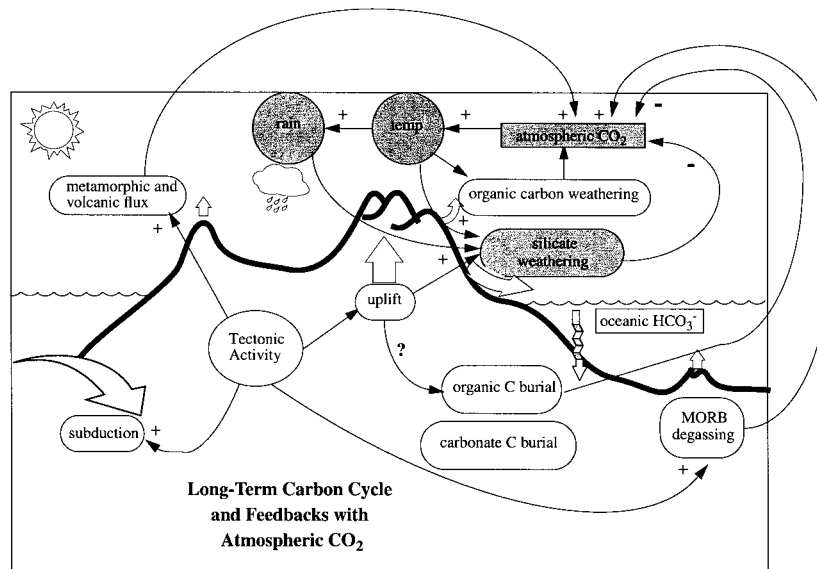


**Figure 1** The long-term carbon cycle, highlighting feedback loops in the carbonate-silicate subcycle that potentially regulate atmospheric  $p\text{CO}_2$  and climate. Arrows with a + symbol near the arrow head represent positive couplings, for which the sense of the change is the same in both connected system components; the negative couplings (with a – near the arrow head) represent couplings where the sense of change is opposite in the component at the arrow's head. Rectangles represent carbon reservoirs, ovals represent important processes, and circles represent important parameters. Hollow arrows represent material transport.

$p\text{CO}_2$ , either directly or indirectly, include organic productivity (which ultimately leads to organic carbon burial) and carbonate and silicate weathering. Carbonate and silicate weathering rates also depend on a number of factors discussed later in this article, and these also cannot be considered independent of climate and atmospheric  $p\text{CO}_2$ . Clearly, a systems approach is necessary to develop a better understanding of the interworkings of these various processes.

The relationship between tectonic uplift, weathering, and climate is the subject of a recent collection of papers edited by Ruddiman (1997). Therefore, we will instead devote the bulk of this paper to the links among  $\text{CO}_2$ , climate, and weathering, in an effort to assess the efficacy of the climate-weathering feedback. Laboratory experiments have established a clear dependence of mineral dissolution rate on temperature. We review recent work in this field of mineral dissolution kinetics, and discuss how these studies can be extrapolated to natural weathering

systems. Several attempts have been made to detect a signal of the temperature dependence of weathering in composition and flux data from modern rivers. However, the direct effects of temperature are often obscured by other factors that covary with it. In contrast, many studies document a strong link between riverine discharge and elemental flux, which emphasizes the importance of the hydrological cycle in controlling the chemical erosion rate. We show that effective feedback requires that the rate-limiting step in the consumption of CO<sub>2</sub> during weathering can be a process that is sensitive to CO<sub>2</sub>, albeit indirectly through the dependence of chemical weathering and erosion rates on temperature and net rainfall. We conclude that a combination of tectonics, atmospheric CO<sub>2</sub> variation, and attendant changes in temperature and the hydrological cycle have been the primary influence on chemical erosion rates, and thus the stabilizing influence on climate over Earth's history.

## MINERAL DISSOLUTION IN THE LABORATORY AND IN THE FIELD

The relationship between climate and chemical weathering in nature is complex. Weathering rates depend on factors such as the mineralogy of the rocks exposed, the reactive surface area of these minerals, the supply of water, its residence time in the soil and initial pH, the abundance of organic acids, and the temperature of soil solutions. Decades of laboratory experimentation have been dedicated to the systematic determination of the rate-dependence of weathering on these factors. The database of rate constants for dissolution of primary silicate minerals that has been generated has considerably improved our ability to generate models of weathering (White & Brantley 1995) and models to predict kinetic parameters (e.g. Sverjensky 1992). Dissolution rates for silicates are typically reproducible to within +0.25 log units within one laboratory, and to within two orders of magnitude among different laboratories (see figures 2 and 3 in Brantley & Chen 1995). In addition, although many authors have concluded that the prediction based on laboratory studies of kinetics in field systems is poor, the discrepancy is on the order of one to two orders of magnitude (Schnoor 1990, Swoboda-Colberg & Drever 1993, Yau 1999), and probably within the error of the estimation. And, although the magnitudes of dissolution rates are not precisely constrained, the form of the rate equation is fairly well accepted. Laboratory dissolution rates, though consistently slower than field rates, can therefore shed light on global patterns of weathering.

One way to test the relevance of the database to field observations is to compare the relative rates of dissolution in laboratory and field (Velbel 1993). Many soil investigators have observed a generally reproducible weathering series which predicts that the dissolution rates of minerals decrease in the order olivine > Ca-plagioclase > pyroxene > Na-plagioclase > K-feldspar > muscovite > quartz

(e.g. Krauskopf 1979, Berner & Berner 1996). A graphical compilation of dissolution rates for these minerals as measured in the laboratory at 25°C and pH 5 shows that laboratory measurements generally predict the relative rates of weathering of silicates as observed in natural systems (Figure 2). The few discrepancies can be explained. For example, Fe-containing olivine, which is more common than the endmember forsterite in real systems, dissolves faster than forsterite and (by inference) plagioclase—which is also more Na-rich and therefore slower dissolving than the anorthite endmember. The discrepancy with respect to albite and potassium feldspar is probably related to the affinity of soil solutions (see discussion about affinity later in this section). Soil solutions are also commonly oversaturated with respect to quartz, which explains the relatively slow observed rates of dissolution of this phase in soils. Overall, the relative rates are consistent among field and laboratory systems.

What explains the general weathering trend, sometimes known as the Goldich series? In this section, we review model equations for mineral dissolution rates, and in particular the rates of dissolution of feldspars, inosilicates, and orthosilicates—the phases that are most important in the long-term drawdown of CO<sub>2</sub> from the atmosphere. We discuss (1) mineral composition, (2) mechanism of dissolution, (3) temperature of dissolution, (4) effects of electrolytes and organic chemistry of dissolving solutions, (5) effects of chemical affinity of dissolving

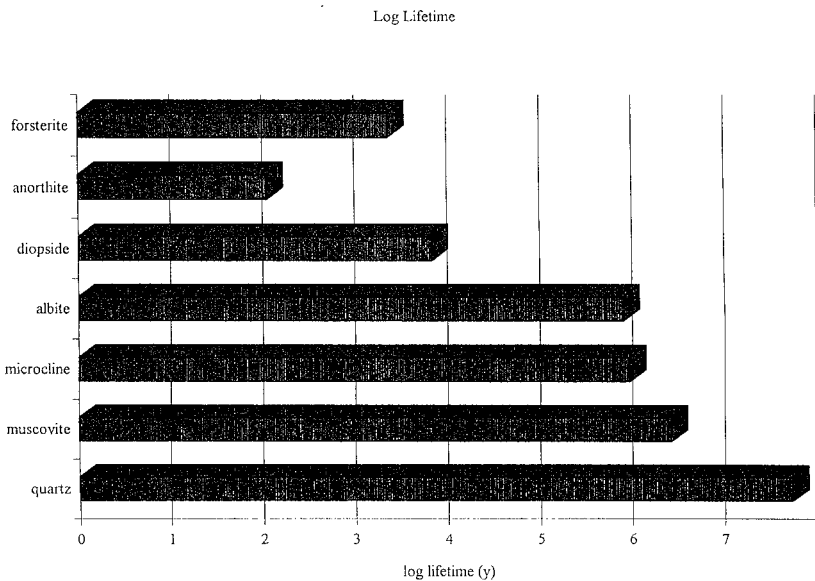


**Figure 2** Graphical representation of log (lifetime) of a theoretical 1 mm diameter crystal at pH 5, 25°C, in dilute solution (after Lasaga et al 1994, with more recent estimates of dissolution rates).

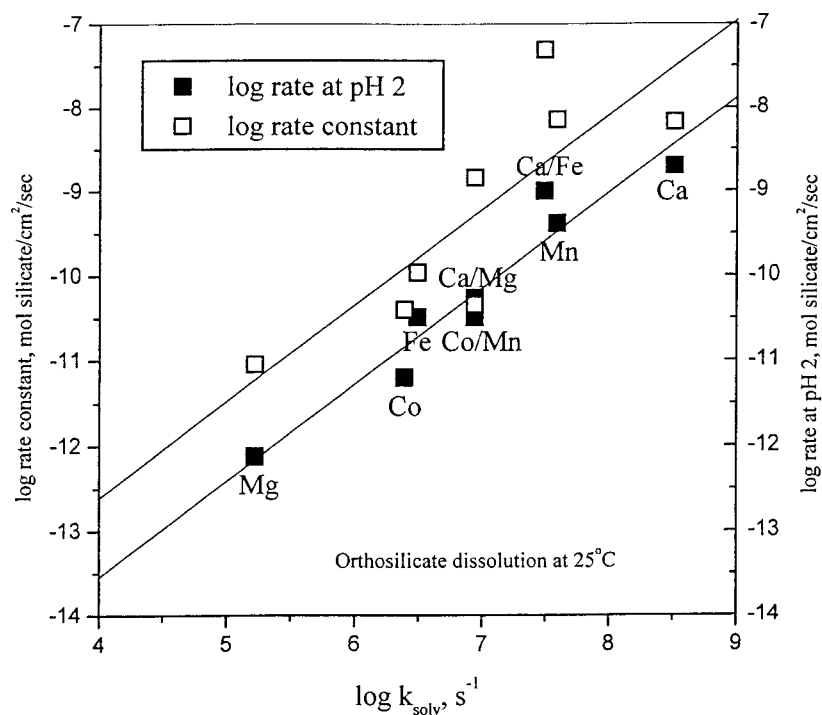


**Figure 3** Correlation between log dissolution rates of orthosilicates and rates of solvent exchange of divalent cations (after Westrich et al 1993). Values of  $\log k_{\text{solv}}$  are taken from Hewkin & Prince (1970).

solutions, (6) the importance of reactive surface area of the dissolving phase and the duration of dissolution, and (7) biological factors.

## Mineral Composition

For dissolution of most silicates in acidic solutions, the rate of release of elements to solution ( $r$ , mol s<sup>-1</sup>) can be modeled as a function of the surface area of the dissolving mineral,  $A$ , and the activity of hydrogen ion,  $a_{\text{H}^+}$ :

$$r = kA(a_{\text{H}^+})^n. \quad (1)$$

Here  $k$  is the rate constant (mol silicate/cm<sup>2</sup>/sec) and  $n$  (unitless) is the apparent reaction order with respect to the  $\text{H}^+$  activity ( $a_{\text{H}^+}$ ). For most soils,  $a_{\text{H}^+}$  is controlled by  $p\text{CO}_2$ , mineral and organic acids, and dissolution/precipitation reactions.

The rate of dissolution of most oxides is slowest in solutions where  $\text{pH} = \text{pH}_{\text{ppzc}}$ , the pH where the surface charge of the mineral of interest (due to sorption

of  $H^+$  and  $OH^-$ ) equals zero. Thus, Equation 1 describes dissolution below the  $pH_{ppzc}$  for any mineral. Close to the  $pH_{ppzc}$ , the rate of dissolution of oxides shows no  $pH$  dependence, and above the  $pH_{ppzc}$ , oxides typically show enhanced dissolution. For most common primary silicates except quartz, the  $pH_{ppzc}$  is thought to equal 5 or above (Sverjensky 1994). Rate equation (1) therefore is useful for any acidic or slightly acidic weathering system. Even for the alkali feldspars where the  $pH_{ppzc}$  is lower than 5 (e.g. Sverjensky 1992), Equation 1 describes the dissolution rate for  $pH$  conditions  $\leq 5$ .

Westrich et al (1993) found that the dissolution rates of orthosilicates at  $pH$  2 and  $25^\circ C$  are correlated with  $k_{solv}$ , the rate constant of exchange of  $H_2O$  molecules bound to the corresponding hydrated, divalent cation in solution. It is expected, therefore, that a similar correlation exists between  $k_{solv}$  and the rate constant of orthosilicate dissolution using model Equation 1. Using data from Westrich et al (1993), the rate constants for the orthosilicates can be regressed versus  $k_{solv}$  (see Figure 3) to yield:

$$\log k_o = 1.13 \log k_{solv} - 17.13. \quad (2)$$

For comparison, the original data of Westrich et al (1993) for log rate (mol silicate/cm<sup>2</sup>/sec) measured at  $pH$  2 are also plotted. Using the same approach, Banfield et al (1995) showed that the log rates for inosilicates also correlate with  $\log k_{solv}$ , although the correlation is not as good as for orthosilicates. Thus, to first order, some of the Goldich weathering series is determined by the value of  $k_{solv}$  for the corresponding cation (Table 1).

**TABLE 1** Value of  $k_{solv}$  and predicted dissolution rate constants based on Equation 2.<sup>a</sup>

M	$\log k_{solv}^b$ ( $sec^{-1}$ )	$\log k_o^c$ (mol silicate/cm <sup>2</sup> /sec)		
		ortho- <sup>d</sup>	single-chain <sup>e</sup>	double chain <sup>f</sup>
Ca	8.5	-7.5	-11.8	-13.4
Mn	7.6	-8.5	-12.8	-14.4
Zn	7.5	-8.7	-13.0	-14.6
Fe	6.5	-9.8	-14.1	-15.7
Co	6.4	-9.9	-14.2	-15.8
Mg	5.2	-11.3	-15.6	-17.2
Ni	4.4	-12.2	-16.5	-18.1
Be	3.5	-13.2	-17.5	-19.1

a. Values listed are log (rate constants) of ortho- and inosilicate hypothetical end-members. Some end-members may not exist in nature. Rate constants for mixed composition silicates can be calculated as weighted averages of log rate constants of the end members.

b. Data from Hewkin & Prince (1970).

c. Log (rate constant) at  $25^\circ C$ .

d. Orthosilicates of composition  $M_2SiO_4$ .

e. Single-chain inosilicates of composition  $M_2Si_2O_6$ .

f. Double-chain inosilicates of composition  $M_7Si_8O_{22}(OH)_2$ .

In spite of the foregoing generalization, not all Ca-containing silicates dissolve more rapidly than Mg-containing silicates, as would be predicted by Table 1. Rate constants measured for an inosilicate are slower than those measured for the corresponding orthosilicate, which suggests that rate inversely correlates with polymerization of silicon-oxygen tetrahedra. The slope of lines on a plot of the log rate constant (mol Si release/cm<sup>2</sup>/sec) versus bridging oxygen per tetrahedron plot varies from -1.7 to -2.6 for different cations (Figure 4). An average slope of -2 is defined by all the data and used for prediction purposes here.

Using the relations shown in Figures 3 and 4, the rate constants for dissolution of the orthosilicates and inosilicates in terms of connectedness ( $C$ ) and  $k_{\text{solv}}$  can be expressed as follows:

$$\log k_o = \log (10_{\text{solv}}^{-2C + 1.13 \log k - 17.13/n_{\text{Si}}}). \quad (3)$$

Here,  $k_o$  is the rate constant at 25°C for the rate model expressed in Equation 1

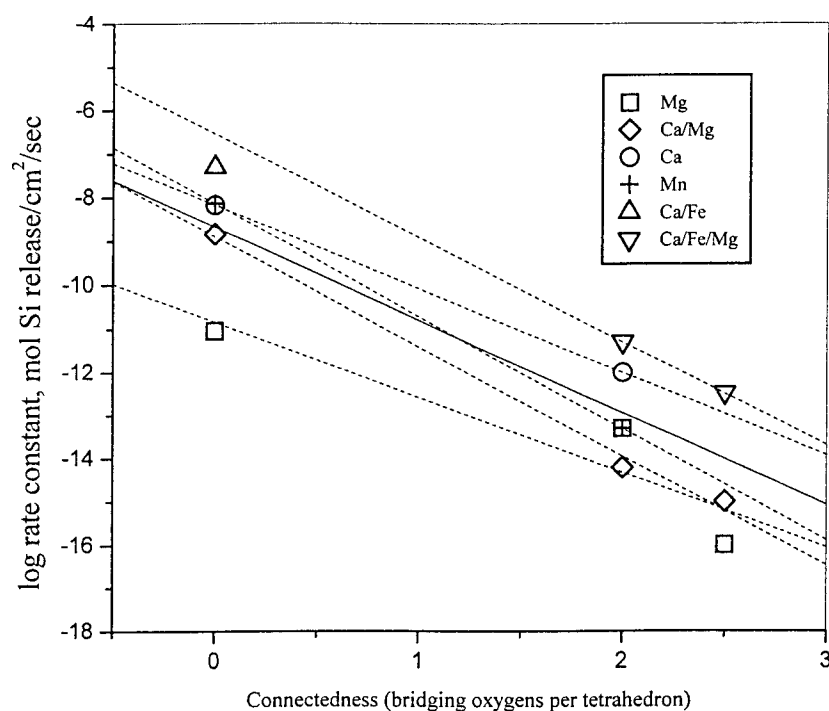


**Figure 4** Relation between log rate constant of Si release and connectedness. Connectedness is defined as the number of bridging oxygens per tetrahedron. Connectedness equals 0 for orthosilicates, 2 for single-chain silicates, and 2.5 for double-chain silicates. An average slope of 2 is obtained based on linear regression of all data. The slopes of the individual lines are: Mg =  $1.7 \pm 0.7$ , Ca/Mg =  $2.5 \pm 0.2$ , Ca = 1.9, Mn = 2.6, Ca/Fe/Mg = 2.4. (See Brantley & Chen 1995 for data sources.)



(in mol silicate/cm<sup>2</sup>/sec), and  $n_{\text{Si}}$  is the number of Si atoms in the mineral formula, e.g.  $n_{\text{Si}} = 2$  for pyroxene, and  $n_{\text{Si}} = 8$  for amphibole.

To further parameterize Equation 1, the value of  $n$  can be bracketed by observing that most published data for inosilicates derived from long-duration dissolution experiments (> one month) vary from 0.2 to 0.4 (see Table 5 in Brantley & Chen 1995). An average value of 0.3 for the reaction order with respect to H<sup>+</sup> is therefore chosen as the representative value for pyroxene and amphibole dissolution. The rate equation for inosilicate dissolution thus yields:

$$\log r = \log (10_{\text{solv}}^{-2C+1.13\log k-17.13/n_{\text{Si}}}) - 0.3\text{pH} + \log A. \quad (4)$$

A general equation such as Equation 4 has not yet been parameterized for feldspar dissolution. Instead, an extended rate equation has been parameterized for feldspars:

$$r = A(k_{\text{H}^+}(a_{\text{H}^+})^n + k_{\text{H}_2\text{O}} + k_{\text{OH}^-}(a_{\text{OH}^-})^p). \quad (5)$$

Here,  $k_{\text{H}_2\text{O}}$  is the rate constant for dissolution under neutral pH,  $k_{\text{OH}^-}$  is the rate constant under basic pH,  $a_{\text{OH}^-}$  is the activity of the hydroxyl ion, and  $p$  is a constant for a given mineral. More mechanistic rate laws incorporating surface complexation have also been developed, but for modeling chemical weathering at the global scale, Equation 5 is more than adequate.

Equation 5 generally predicts that log (dissolution rate) versus pH has a V-shape, with the trough of low dissolution rate occurring at pH = pH<sub>ppzc</sub>. Parameters for Equation 5 for feldspar minerals are summarized in Table 2; however, the value of the rate constants appropriate at neutral and basic pH ( $k_{\text{H}_2\text{O}}$ ,  $k_{\text{OH}^-}$ ) have not been well constrained, and are therefore only listed for albite and potassium feldspar. One problem in constraining the rate of dissolution of feldspar under neutral pH is that dissolution is so slow under neutral conditions that rates

**TABLE 2** Measured rate parameters at 25°C for feldspar minerals.

	$\log k_{\text{H}^+}$ mol m <sup>-2</sup> s <sup>-1</sup>	$\log k_{\text{H}_2\text{O}}$ mol m <sup>-2</sup> s <sup>-1</sup>	$\log k_{\text{OH}^-}$ mol m <sup>-2</sup> s <sup>-1</sup>	$n$	$m$	$p$	pH <sub>ppzc</sub> <sup>a</sup>	$E^{\text{a}}$ kJ mol <sup>-1</sup>
Microcline	-9.9– -9.4	—	-10.4– -9.2 <sup>b</sup>	0.4–0.5 <sup>b</sup>	—	0.3–0.7 <sup>b</sup>	6.1	-60 <sup>b</sup>
Albite	-9.7– -9.5 <sup>b</sup>	-12.2– -9.4 <sup>b</sup>	-9.9 <sup>b</sup>	0.5 <sup>b</sup>	0 <sup>c</sup>	0.3 <sup>b</sup>	5.2	-60 <sup>b</sup> -65 <sup>c</sup>
Labradorite	-9.9– -9.4 <sup>b</sup>	—	—	0.4–0.5 <sup>b</sup>	—	—	—	-60 <sup>b</sup>
Anorthite	-9.9– -9.4 <sup>b</sup>	—	—	0.9–1.1 <sup>b</sup>	—	—	5.6	-80 <sup>b</sup>

a. Values of the pristine point of zero change are from calculations summarized by Sverjensky (1994). Values of pH<sub>ppzc</sub> for feldspars may be significantly lower than these quoted values, depending on the model used for calculation and on the degree of proton-exchange of the surface.

b. Blum & Stillings 1995.

c. Chen & Brantley 1997.

may be unmeasurable in laboratory time frames. In fact, many workers have set the second term equal to zero in Equation 5, and included only the proton-promoted and hydroxyl-promoted terms. Slow rates under neutral conditions emphasize the importance of natural acids in mineral weathering; dissolution under neutral pH is orders of magnitude slower than dissolution in acid conditions (Figure 5).

## Mechanism of Dissolution

To extrapolate a rate of dissolution confidently from one system to another, the rate of an elementary reaction must be known, and the same reaction must control the rate in the new system. An elementary reaction occurs at the molecular level, exactly as written. In geochemistry, few mechanisms, not to mention rates, of

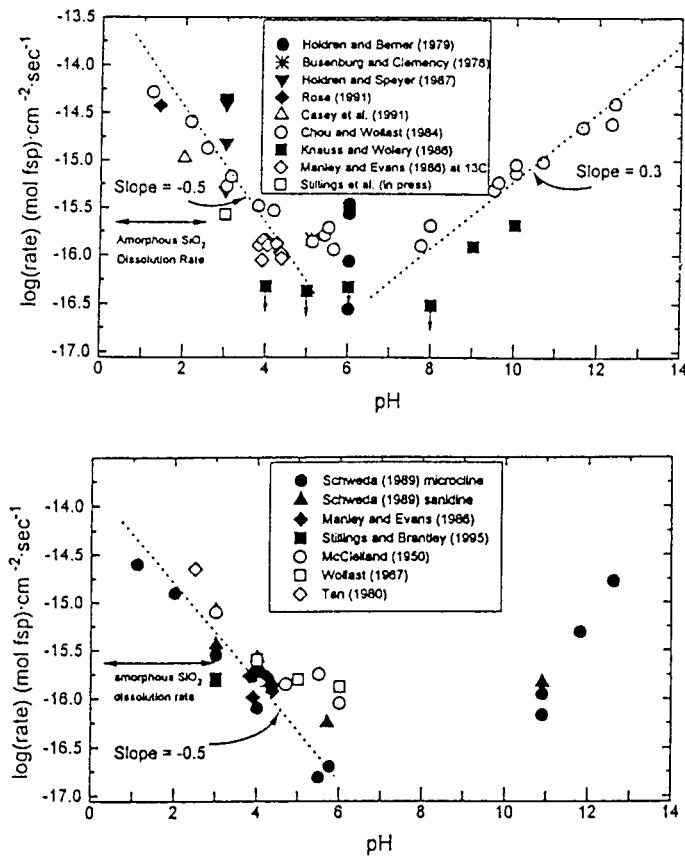


**Figure 5** Feldspar dissolution rates as a function of pH. Data separated into two plots for clarity. After Blum & Stillings (1995), who provide references for legend.

elementary reactions are known. For example, Murphy et al (1998) demonstrated that the rate of dissolution of biotite in laboratory systems was three to four orders of magnitude faster than the rate of weathering in a well-characterized saprolite in Puerto Rico. However, it is probable that the biotite had weathered to an inter-layered vermiculite-biotite in laboratory experiments, whereas in the field, biotite weathered to kaolinite. The difference in mechanism can therefore explain some of the discrepancy between laboratory and field in that study.

Reactions that are interface-limited in the laboratory may be transport-limited in the field. Transport limitation can include limitation by slow advection or diffusion of reactants to, or of products away from, the site of reaction. However, Berner (1978, 1981) has pointed out that the rate of diffusion is fast enough that rate limitation by diffusion through soil pore fluids is inconsistent with retention of silicates in soils for thousands to millions of years.

For fast-dissolving phases such as evaporite minerals, or for reactions at high temperatures, many authors have assumed that transport becomes rate-limiting in field systems (Berner 1981). On the other hand, for dissolution or precipitation of silicates at ambient conditions, most authors have assumed that the interface reaction is rate-limiting. Few field studies have documented unequivocally the nature of the rate-limiting step, however. One common argument has been the identification of rounded crystal surfaces with transport-limited dissolution (e.g. rounding of calcite reported by Berner 1978) and of etched crystal surfaces with interface-limited dissolution (etched feldspars, pyroxenes, and amphiboles summarized in Berner & Berner 1996). Another argument in favor of the interface reaction controlling silicate dissolution derives from the generally convincing comparison, presented previously, of the relative rates of weathering in the field and in the laboratory (Figure 2). Furthermore, the observation of differences in weathering rates for different phases is consistent with some degree of interface control.

However, Schnoor (1990) argues that Si release (equated to weathering rate) increases to a maximum value comparable to release rates measured in silicate dissolution rates in the laboratory as the soil flushing rate (ratio of flow-rate to soil mass) increases. Schnoor (1990) argues that for low values of the flow-rate-to-mass ratio, transport limits weathering, but at values of flushing rate higher than approximately 1.0 volume of water per volume of soil per day, the interface reaction becomes rate-limiting. According to Schnoor, the lower flushing rates of field systems can account for the lower Si release rates observed during field weathering. The argument of Schnoor is supported by data worldwide, as plotted in Figure 6 from Holland (1978); Holland's data suggests that increased flushing rates above a certain value do not increase concentrations of dissolved solids for rivers worldwide, but rather lead to dilution. Therefore, weathering may be transport-limited at low flushing rates and interface-limited at high flushing rates. Because the largest dissolution flux derives from high runoff sites, silicate weathering is probably controlled by interface-limitation globally.

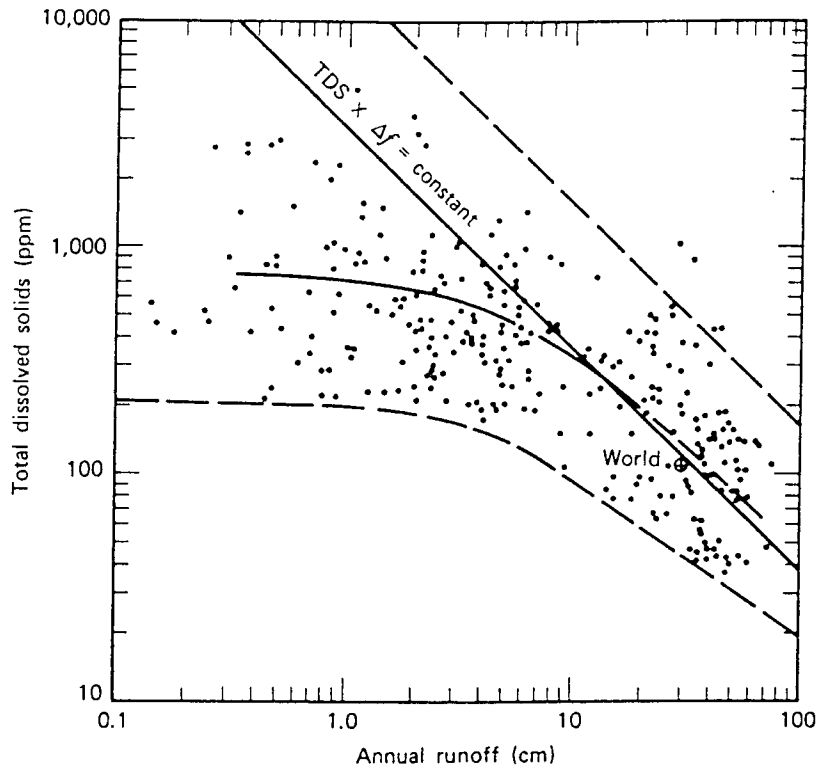


**Figure 6** Holland's (1978) plot of total dissolved solids vs. runoff for the world's rivers. Solid curve shows general trend; solid line shows dilution trend.

A simple model (after Berner 1978) is consistent with Figure 6. With  $F$  = flushing volume per unit time,  $V$  = volume of water in a weathering system,  $R$  = mass dissolved per unit volume solution per unit time,  $c$  = concentration of solute  $i$ , and  $t$  = time, conservation of mass requires:

$$\frac{\partial c}{\partial t} = R - \frac{F}{V} c. \quad (6)$$

If net dissolution rate slows as  $c$  approaches  $c_{eq}$  (equilibrium solubility), and if  $R = k(1 - c/c_{eq})$  where  $k$  is the rate constant, then at steady state,

$$c = \frac{kc_{eq}}{k + k_f c_{eq}} \quad (7)$$

and

$$R = k \frac{k_f c_{eq}}{k + k_f c_{eq}} \quad (8)$$

where  $k_f$  is the flushing frequency or residence time ( $= F/V$ ). As  $F$  (or  $k_f$ ) increases,  $c$  and  $R$  decrease and increase respectively. Dissolution rates should therefore increase in a soil with increasing runoff. However, at high  $k_f > k$ ,  $c$  approaches  $\frac{k}{k_f}$  and the rate approaches  $k$ , independent of flushing rate. Similarly, for  $k_f \ll k$ ,  $c$  approaches  $c_{eq}$ , and  $R$  approaches  $k_f c_{eq}$ . The form of these equations thus predicts the form of the data in Figure 6. However, other hydrological factors affect concentration-runoff relationships for streams—including activation of alternative flowpaths and increase in contributing areas during storms (e.g. Richards 1999)—so this simple extension of the model of Berner 1978 should be considered a first-order approach. We will return to an analysis of concentration-runoff relationships in discussing controls on chemical erosion rates later in this article.

## Temperature of Dissolution

One way to investigate the rate-limiting step of a reaction mechanism is to assess the activation energy. For example, the values of rate constants vary with temperature according to the Arrhenius equation:

$$k = k' e^{-E_a/(RT)}, \quad (9)$$

where  $k'$  (mol silicate/cm<sup>2</sup>/sec) is the temperature-independent, pre-exponential factor,  $E_a$  is the activation energy,  $R$  is the gas constant, and  $T$  is the absolute temperature (Laidler 1987). If a mineral-water reaction is rate-limited by diffusion through water, then the  $E_a$  is the activation energy of diffusion ( $= 4\text{--}5$  kcal/mol); similarly, if the process is rate-limited by advection, then the  $E_a$  is that of the kinematic viscosity and is slightly less than the value for diffusion (Berner 1978).

Values of the  $E_a$  for dissolution of silicates are much larger than the  $E_a$  for diffusion or advection. However, studies have shown that  $n$  in Equation 1 or 5 can also be temperature-dependent, affecting the apparent  $E_a$  (the  $E_a$  observed when rates are compared for any  $\text{pH} \neq 0$ ). According to Casey & Sposito (1992) and Brady & Walther (1992), for  $\text{pH} < \text{pH}_{\text{ppzc}}$ , an increase in temperature will result in an increase in  $n$  in Equation 5. The increased value of  $n$  at higher temperature has been observed by experiments for silicates (e.g. kaolinite, Carroll-Webb & Walther 1990; inosilicates, Chen & Brantley 1998). For other minerals, however, controversy exists as to whether  $n$  varies or remains constant with temperature [for albite, compare Hellmann (1994) and Chen & Brantley (1997); for orthosilicates, compare Casey et al (1993), Chen & Brantley (1999), and Rosso & Rimstidt (1999)]. For phases where  $n$  increases with temperature, activation energies reported in Table 3 are larger than the observed  $E_a$  for rates compared at any  $\text{pH} > 0$ .

**TABLE 3** Parameters for rate estimation for ortho- and inosilicates.

	Connectedness <sup>a</sup>	$n_o$ <sup>b</sup>	$m^c$ (/K)	$E_a^d$ (kcal/mol)	pH <sub>ppzc</sub> <sup>e</sup>
Orthosilicates	0	0.5	0.0062	22	4.9–10.4
Single-chain Silicates	2	0.3	0.0088	21	5.9–8.5
Double-chain Silicates	2.5	0.3	0.0060	19	6.6–7.0

a. Number of bridging oxygens

b. Reaction orders with respect to H<sup>+</sup> at 25°C

c. Rate of change in  $n$  with respect to temperature

d. Activation energy of dissolution

e. From the compilation by Sverjensky (1994). Note that some of these values are dependent on the model used for calculation (e.g. see Parks 1967).

Because  $n$  can vary with temperature, two kinds of  $E_a$  are cited in the literature: a pH-dependent activation energy, and a pH-independent activation energy (Brantley & Chen 1995). The pH-dependent activation energy,  $E_a'$ , is reported by investigators who determine the value of  $E_a'$  based upon an Arrhenius plot of  $\ln$  (rate at pH  $x$ ) vs.  $1/T$ . This  $E_a'$  is valid only at the pH of measurement. The pH-independent  $E_a$  (Equation 9) is determined from a plot of  $\ln$  (rate constant) vs.  $1/T$ . These two values of  $E_a$  are not equal if  $n$  varies with temperature. Where  $n$  is independent of temperature, then  $E_a' = E_a$ .

For silicates where  $n$  varies with  $T$ , the rate of change in  $n$  can be modeled with a linear dependence on temperature:

$$m = (n - n_o)/(T - T_o) \quad (10)$$

where  $n_o$  is the value of  $n$  at temperature  $T_o$ . Combining Equations 5, 9, and 10 and setting  $T_o = 298.15$  K, a general rate equation for silicates can be written:

$$r = k_o e^{(E_a/R)(1/298.15 - 1/T)} (a_{H^+})^{m(T - 298.15) + n_o} \quad (11)$$

or

$$\log r = \log k_o + [E_a/(2.303R)](1/298.15 - 1/T) - [m(T - 298.15) + n_o]pH \quad (12)$$

where  $k_o$  is the rate constant at 25°C and  $n_o$  is the reaction order with respect to H<sup>+</sup> at 25°C. This rate equation is predicted to be valid for values of pH < pH<sub>ppzc</sub> for silicate minerals.

For feldspars (assuming  $m = 0$  by analogy to albite), parameters for Equation 12 are summarized in Table 2. For these phases,  $E_a$  is constant with pH. However, accepting the theoretical prediction that  $n$  increases with temperature (Casey & Sposito 1992, Brady & Walther 1992) for orthosilicates and inosilicates, and using the data compiled for orthosilicates (Casey et al 1993, Westrich et al 1993, Chen & Brantley 1999) and inosilicates (Chen & Brantley 1998), the values of 0.0062,

0.0088, and 0.0060 K<sup>-1</sup> (see Table 3) can be chosen as representative values of  $m$  (Equation 10) for orthosilicate, pyroxene, and amphibole dissolution, respectively.

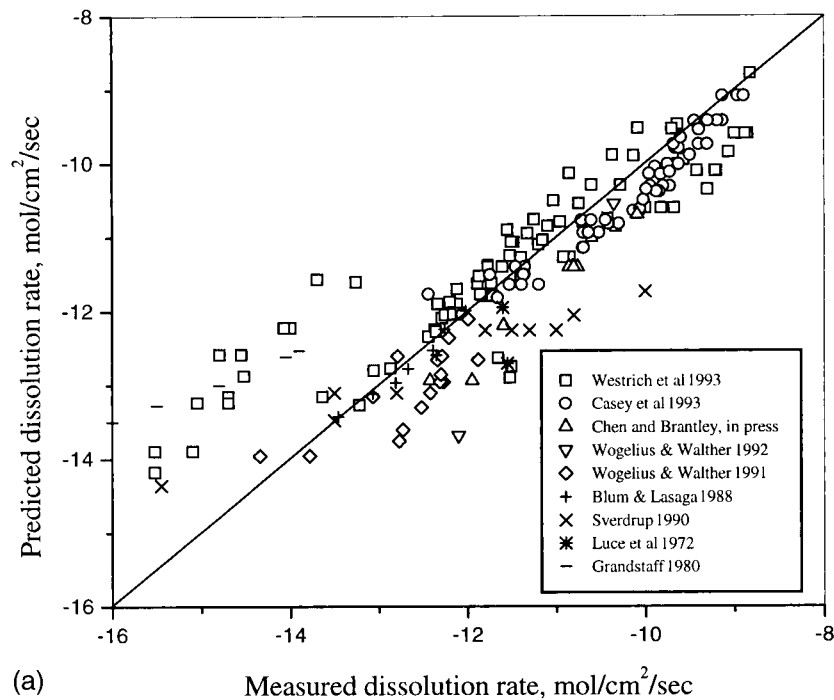
Values of  $E_a$  are still relatively poorly defined, and for the orthosilicates and inosilicates, variations in  $E_a$  as a function of composition and connectedness are not well known. A value of 22 kcal/mol is probably acceptable as an  $E_a$  for orthosilicate dissolution; this estimate is based on values measured by Casey et al (1993), Westrich et al (1993), and Chen & Brantley (1999). Literature data on the activation energy of dissolution for pyroxenes are inconsistent and range from 9 to 36 kcal/mol (Brantley & Chen 1995), but an estimated value of 21 kcal/mol (Table 3) can be used to represent the activation energy for the single-chain silicates. The only data available for double-chain silicates is for anthophyllite dissolution at temperatures of 25° and 90°C (Chen & Brantley 1998). The value of 19 kcal/mol from that work is therefore chosen to represent the activation energy of double-chain silicate dissolution.

Using these parameters, dissolution rates of end-member and mixed cation ortho-, single-chain, and double-chain silicates predicted using Equation 12 are plotted against measured rates in Figure 7. Figure 7 shows that Equation 11 predicts rates within one to two orders of magnitude of measured rates for most ortho- and single-chain silicates. Such agreement is reasonable considering the large discrepancies in measured dissolution rates in the literature, which often differ by one or two orders of magnitude for the same mineral under similar conditions. The best predictions (generally within an order of magnitude) are made for the orthosilicates. The largest discrepancy for these phases occurs for the Ni-olivine composition (Westrich et al 1993) and data for forsterite by Grandstaff (1980). However, the rates reported by Grandstaff (1980, 1986) are one to two orders of magnitude lower than the rates reported later for forsteritic olivine and other orthosilicates at similar temperature and pH conditions (e.g. Blum & Lasaga 1988, Sverdrup 1990, Wogelius & Walther 1991, Westrich et al 1993, Chen & Brantley 1999). Some of this discrepancy may have been related to an erroneously measured BET surface area (as suggested by Murphy 1985; Wogelius & Walther 1991, 1992). Predictions are poorer for the pyroxenes and amphiboles. However, the rate equation provides model rates within a factor of 100 of measured values for most data for pyroxene dissolution. The lack of amphibole data makes evaluation of this model equation impossible, and parameterization of this equation should be seen as preliminary at best. For the orthosilicates and single-chain silicates, however, Figure 7 should allow distinction between consistent rate measurements and those that may be in error.

Table 3 can also be used to estimate  $E_a'$  at common values of soil pH. To calculate  $E_a'$  (pH =  $x$ ) from  $E_a$  in Table 3, the estimated value of  $m$  is used in the following equation:

$$E_a'(\text{at pH} = x) = (\log(k_1/k_2) + (n_2 - n_1) x)2.303 R/(1/T_2 - 1/T_1) \quad (13)$$

## Orthosilicate Dissolution Rates

(a) Measured dissolution rate, mol/cm<sup>2</sup>/sec

**Figure 7** Comparison between observed and model-predicted rates of silicate dissolution. (a) Orthosilicates; (b) Pyroxene; (c) Amphibole.

In this equation,  $x$  is the pH for which  $E_a$  is calculated,  $k_1$  and  $k_2$  are rate constants for Equation 1 measured at two temperatures,  $T_1$  and  $T_2$ , or calculated from Equation 12, and  $n_1$  and  $n_2$  are the values of  $n$  for those two temperatures.

## Electrolyte and Organic Chemistry of Dissolving Solutions

Often, groundwater or soil porewater chemistry differs from the chemistry of laboratory solutions used for kinetic experiments. Correcting for discrepancies in inorganic solution chemistry may revise dissolution estimates in the field by relatively small factors (typically  $< 5$ ). The presence of dissolved alkali cations in solution has been observed to decrease the rate of dissolution of feldspars (Stillings & Brantley 1995). These workers modeled inhibition of feldspar dissolution by the presence of dissolved  $Na^+$  using a competitive adsorption model:

$$R = kN_s \left[ \frac{K_H a_{H^+}}{1 + k_H a_{H^+} + K_{Na} a_{Na^+}} \right]^{0.5} \quad (14)$$



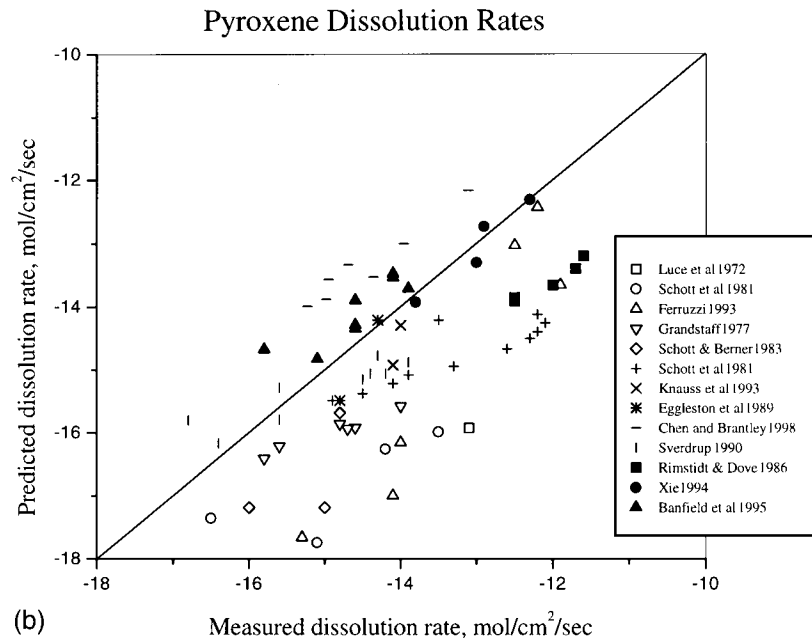


**Figure 7** Comparison between observed and model-predicted rates of silicate dissolution. (a) Orthosilicates; (b) Pyroxene; (c) Amphibole.

where  $R$  is the dissolution rate ( $\text{mol cm}^{-2} \text{s}^{-1}$ ),  $N_s$  is the density of adsorption sites,  $K_H$  is the equilibrium constant for adsorption of  $H^+$  at the mineral surface, and  $K_{Na}$  is the equilibrium constant for adsorption of  $Na^+$  at the mineral surface. Values for these parameters were summarized in the original article.

No such model for the effect of alkali cations in solution has been proposed for the dissolution of ortho- or inosilicates where the effect of differences in solution chemistry other than pH on rate has been generally reported as small (see Brantley & Chen 1995, Chen & Brantley 1999, and references therein). Similarly, no general model for the effect of anions in solution (other than  $\text{OH}^-$ ) have been proposed, and the effect of inorganic anions may be minor on the rates of dissolution of both ortho- and inosilicates (see Brantley & Chen 1995, Chen & Brantley 1999, and references therein). It is probable, however, that increasing dissolved alkali salts in weathering solutions will generally result in decreased dissolution rates, although corrections will be relatively small.

The effect of dissolved Al has also been investigated for several phases. In general, dissolved Al inhibits dissolution of aluminosilicates (e.g. Gautier et al 1994, Brantley & Chen 1995), perhaps because of adsorption on the mineral surface. However, the inhibitory effect of dissolved aluminum may be larger at temperatures above ambient. Distinguishing the effect on dissolution of dissolved

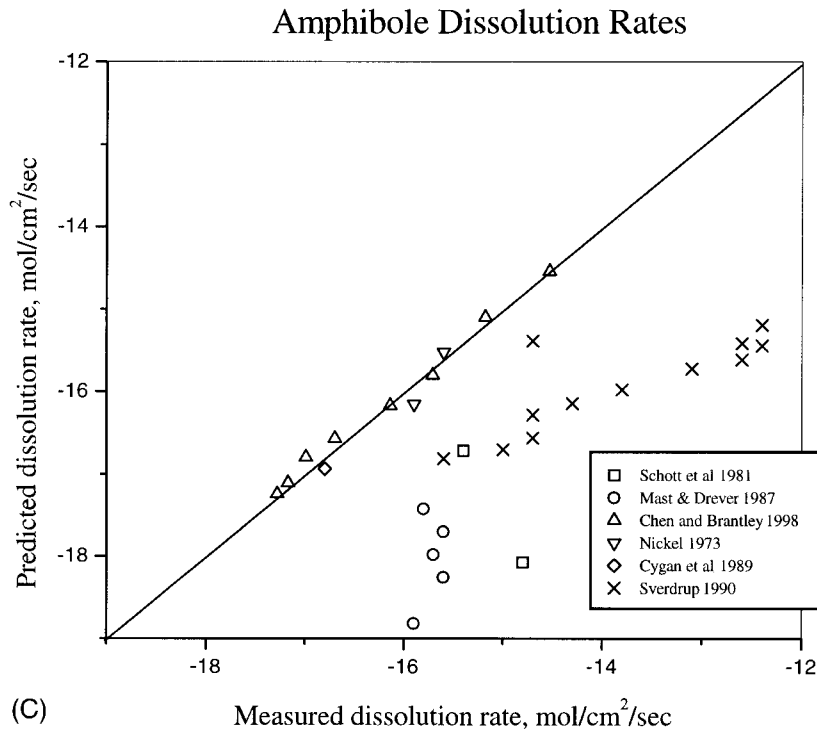


**Figure 7** Comparison between observed and model-predicted rates of silicate dissolution. (a) Orthosilicates; (b) Pyroxene; (c) Amphibole.

aluminum from an affinity effect for rates of dissolution of aluminosilicate is controversial (e.g. Burch et al 1993, Lasaga et al 1994, Gautier et al 1994).

The effects of organic acids on alkali- and alkaline-earth-containing silicates has been studied by many workers, though experimental results are confusing. Most of the rate measurements have been completed with oxalic acid, a dicarboxylic acid found in soil solutions. Again, the most definitive work has been completed on feldspars: for example, Stillings et al (1996) reported experiments with a range of feldspar compositions, a range of pH, and a range of oxalic acid concentrations. The dissolution of feldspar increased by a factor of 2–15 in the presence of 1 mM oxalic acid, as compared to rates in inorganic solutions at the same pH. The factor of enhancement of dissolution rate in the presence of oxalic acid over the rate in an inorganic solution of identical pH did not vary as a function of feldspar composition at pH 3, but it may have shown an increase with increasing An content for dissolution at pH 5. The effect of organic acids on weathering of mafic rocks could be greater, therefore, than the effect on granitic lithologies (Drever 1994).

Drever (1994) has pointed out, however, that the effect of organic acids in accelerating the dissolution rates in nature is probably minor because of low concentrations of organics in soil waters. It is also important to note that high concentrations of organic acids occur in soils in cool climates, precisely where weathering rates might be predicted to be slower, based on a temperature effect. Tropical soils, such as the fast-weathering Rio Icacos watershed in Puerto Rico investigated by White & Blum (1995), contain little to no organic acids (Murphy et al 1998). However, some organic molecules such as siderophores are extremely strong chelates and may be important in affecting rates, even if present at extremely low concentrations (Liermann et al 2000).

Very little work has been completed to investigate the direct effect of dissolved  $\text{CO}_2$  on silicate or oxide/hydroxide dissolution. Most laboratory workers have assumed that the effect of  $\text{CO}_2$  on abiotic dissolution could be predicted based on the effect of the dissolved gas on the pH. For certain phases, however, carbonate complexation at the mineral surface might be important. Knauss et al (1993) reported that under alkaline conditions the release of Ca and Mg from diopside during dissolution was enhanced at  $p\text{CO}_2 < \text{atmospheric}$ , and they speculated that Mg and Ca surface sites were poisoned by carbonate complexation, similar to that observed for olivine (Wogelius & Walther 1991). Likewise, at pH 10 and 12, Xie (1994) postulated a surface Ca-carbonate complex to explain an observed decrease in silica release rate of wollastonite in the presence of ambient  $\text{CO}_2$  by about two orders of magnitude as compared to  $\text{CO}_2$ -free NaOH solution. Carbon dioxide also adsorbs strongly to goethite surfaces (Russell et al 1975, Zeltner & Anderson 1988, Van Geen et al 1994), and carbonate complexation has also been used to model the effect of  $p\text{CO}_2$  on hematite dissolution using the surface complexation theory (Bruno et al 1992). Complexation of carbonate at mineral surfaces, especially Fe- and alkaline-earth-containing minerals, may therefore affect dissolution rates. Whether the magnitude of these effects is large enough to be geochemically important is unknown. For example, Brady & Carroll (1994) measured the dissolution rates of augite and anorthite at pH 4 ( $\pm 0.05$ ) and saw no difference in dissolution rate as a function of  $p\text{CO}_2$ .

Brady & Carroll (1994) argue that enhanced levels of  $\text{CO}_2$  in the atmosphere probably accelerates silicate weathering predominantly by acceleration of organic activity. They correctly point out that decreases in soil porewater pH with increased  $p\text{CO}_2$  would have little effect on feldspar weathering at near-neutral pH, because feldspar dissolution rates are roughly independent of pH from 5 to 8. They also correctly point out that organic acids become protonated and less corrosive at lower pH, an effect that would mute the importance of lower pH resulting from high levels of  $p\text{CO}_2$ . However, it is worth pointing out that in tropical watersheds, very little dissolved organic matter is expected in soil water solutions, and the effect of increased  $p\text{CO}_2$  for such systems could be significant.

### Chemical Affinity of Dissolving Solutions

In discussing the effect of flushing rate earlier, we noted that increased flushing will speed up dissolution rate by affecting the affinity term,  $1-c/c_{\text{eq}}$  (note that the

exact form of this affinity term is not well known). At equilibrium, the rates of dissolution and precipitation of a given phase must be identical. As a solution approaches equilibrium from the undersaturated side (as the affinity approaches zero), the rate of precipitation approaches the rate of dissolution, creating a decrease in the net rate of dissolution. Because of slow kinetics, few researchers have measured the rates of dissolution of rock-forming silicates under near-equilibrium conditions and ambient temperatures. However, Burch et al (1993) suggested that if the  $\Delta G$  for albite dissolution was greater than about  $-25$  kJ/mol at  $80^\circ\text{C}$ , then albite dissolution showed a measurable decrease in dissolution rate. Burch et al suggest that dissolution where  $\Delta G < -25$  kJ/mol occurs on the “dissolution plateau” where the rate is constant as a function of affinity. Only a handful of other workers have investigated the effect of affinity on dissolution (for a recent review, see Alekseyev et al 1997). These workers have suggested a variety of affinity terms for incorporation into rate models for oxide and silicate dissolution. Most models predict a dissolution plateau (rate independent of affinity) for undersaturated conditions and an approach to a net rate of zero at equilibrium.

Few researchers have calculated the affinity of weathering solutions. Velbel (1989) used stream and ground water chemistry data from two watersheds and concluded that the affinity term was not important in decreasing the rates of albite weathering in the Blue Ridge Mountains, North Carolina and in Czechoslovakia (Paces 1983, Velbel 1985). In effect, Velbel argued that dissolution in these sites occurs while solutions are in the “dissolution plateau” where rates are not affected by affinity. For these studies, increasing the flushing rate of the system would not be expected to increase the observed rates of weathering because dissolution occurs at the maximum rate already. Increased flushing should just dilute porewaters.

In contrast, Gislason & Arnorsson (1993) observed stream waters and ground waters in Iceland and concluded that in many cases where glass dissolution is significant, dissolution rates of olivine, pyroxene, and plagioclase are slowed because of the near-equilibrium conditions for the mineral phases. For such watersheds, increased flushing (higher rainfall) should increase the observed weathering rates, as Bluth & Kump (1994) reported for many Icelandic watersheds.

Although plagioclase is typically far from equilibrium in soil porewaters, as reported by Velbel (1989), soil porewaters usually reveal that potassium feldspar is closer to saturation in these waters, regardless of the climate and land use characteristics of the system (White 1995). Because feldspar dissolution rate decreases when close to equilibrium, the chemical affinity of soil porewater chemistry probably explains, at least partially, the lower rates of dissolution of potassium-containing feldspar as compared to plagioclase observed in field systems (Figure 2). Thus, the tendency for soils to retain potassium-feldspars while losing plagioclase-feldspars may be partially due to the fact that soil porewaters tend to be closer to equilibrium with respect to K-containing feldspars, as opposed to Na- and Ca-containing feldspars.

## Reactive Surface Area of the Dissolving Phase

Models of weathering in the field and in the laboratory assume that the rate of interface-limited weathering is proportional to the surface area of the reactant mineral (e.g. see Equation 1). Mathematically, the so-called geometric surface area of particles can be calculated from the linear dimensions of the geometric shape of the particles. However, natural surface areas deviate substantially from such geometric models because of surface roughness and porosity. Models that use geometric surface area thus underestimate the total surface area.

For quantitative analysis of surface area for laboratory experiments, geochemists typically use the Brunauer-Emmett-Teller (BET) isotherm (Brunauer et al 1938).

However, the measured surface area comprises both external and internal contributors. Gregg & Sing (1982) point out that the demarcation between the two types of surface area must necessarily be arbitrary, but they defined internal surface area as including all cracks or connected pores which are deeper than they are wide. Hochella & Banfield (1995) proposed that the portion of the surface over which a fluid can flow could be termed external, whereas the grain surface next to which stagnant fluid resides could be termed internal. Therefore, advection can control transport to and away from the external surface, while diffusion must be the transport mechanism for internal pore space.

Porosity has been observed or inferred from adsorption and observational data for both laboratory-ground and field-weathered silicates. In laboratory-ground samples, diopside, hornblende, and all compositions of feldspar except albite have been interpreted to contain internal surface area (Brantley & Mellott 2000). In field-weathered samples, porosity has been observed or inferred in quartz, potassium feldspars, plagioclase, and hornblende (Brantley et al 1999, Brantley & Mellott 2000).

Although most dissolution rate studies have used BET surface area, the surface area measured from the dissolution rate of a solid powder, the reactive surface area (Helgeson et al 1984), differs from the adsorption surface area (White & Peterson 1990). Reasons for the discrepancy may be chemical (e.g. all surface sites on the mineral may not be equally reactive) and physical (e.g. the presence of porosity, which may become transport-limited). Anbeek (1992, 1993) proposed that a distinction should be made between reactive surface area of naturally weathered versus laboratory-ground mineral grains. He argued that most of the new BET surface area created during natural weathering is relatively nonreactive, whereas laboratory-ground surface is highly reactive. Hodson (1999) has argued that much of the BET surface area for some alkali feldspars is a result of grinding-induced microporosity. If such induced surface area does react differently than the surfaces of weathered samples (see, for example, Lee et al 1998), then the BET surface area is an inappropriate parameter to use for extrapolating interface-limited kinetics from laboratory to field (Lee et al 1998, Brantley & Mellott 2000).

For example, if transport in and out of a pore is slow compared to interface-limited reaction within the pore, then solution chemistry in the pore will differ

from bulk chemistry. In the limiting case where an equilibrium assemblage is precipitated within the pore but not outside the pore, reaction inside the pore should be very slow and equal to transport (diffusion) out of the pore. In such a case, using the surface area of the pore to extrapolate interface-limited kinetics is inappropriate.

An additional problem in defining reactive surface area on natural samples is the observation that organic  $\pm$  Fe  $\pm$  Al  $\pm$  Si coatings on natural mineral surfaces may dominate some surface properties (e.g. Davis et al 1993). Davis et al argued that the surface properties of natural quartz/feldspar sand from the glacial outwash of the Cape Cod aquifer (Massachusetts) differs from pristine silicate because of patchy coatings on the grains. Coston et al (1995) concluded that the coating fills surface irregularities that extend several tens of microns into the grain interior, and consists of partially crystalline and microcrystalline material. The exact proportion of the silicate surface that is occluded by the coating is therefore unknown; however, Yau (1999) has shown that this surface coating decreases the *reactive* specific surface area of the aquifer material by about an order of magnitude. This conclusion was based on the observation that removal of the coating caused the release rate of Si from a dominantly feldspar sample to increase by a factor of  $\sim 10$ , after normalization by surface areas. Nugent et al (1998) has shown that development of surface coatings on silicates happens very quickly in temperate soils, and that the coatings are often impossible to image using standard techniques of secondary electron or optical microscopy. If such coatings decrease the reactivity of the surface, then quantification of the chemistry and coverage of such coatings is necessary to predict natural rates of mineral weathering. Quantification of the reactive surface area in a field system—including accounting for the internal surface area and coating coverage—is one of the most difficult remaining questions in geochemical kinetics.

## Important Biological Factors

Few workers have quantified the effect of microbiota or plants on rates and mechanisms of silicate weathering. Despite investigation of the effect of microorganisms on weathering in soil over many years (for a recent review, see Barker et al 1997), observations are generally qualitative rather than quantitative. Proposed mechanisms for dissolution of minerals by lichens, fungi, and bacteria include the use of microbially produced organic or mineral acids (Duff et al 1963, Keil & Schwartz 1980, Barman et al 1992, Bosecker 1993, Barker et al 1997), alkaline metabolites (Aristovskaya & Kutuzova 1968, Kutuzova 1973), polysaccharide slimes (Malinovskaya et al 1990), and chelates (Ullman et al 1996, Liermann et al 2000), as well as oxidation or reduction of metals in the mineral (Ivarson et al 1978, 1979, 1980; Rickard 1973). Almost all of these proposed microbial effects predict enhancement of field weathering rates rather than inhibition. Indeed, most studies emphasize the use of short-chain organic acids and the effect of lower pH and/or enhanced chelation (e.g. Robert & Berthelin 1986). For most minerals,

both a decrease in pH and chelation should increase the weathering rate (White & Brantley 1995). A decrease in weathering rate resulting from microbial action would be hypothesized only for microbial systems excreting alkaline metabolites such as ammonia, certain polysaccharide slimes (Welch & Vandevivere 1994), or armoring crystalline coatings (Urrutia & Beveridge 1994). Presumably, however, the overall effect of microbiology on weathering is an increase in the dissolution rate over purely inorganic systems.

The effects of plants on weathering incorporates both chemical and physical effects. The chemical effects are especially related to the production of organic acids, which affect soil water pH, and which can, in many cases, chelate metal ions and enhance dissolution. Quantification of the impact of excretion of such acids is particularly complex in the presence of plants because microenvironments with bacterial communities are created around plant roots often with associated bacterial communities. In addition, plants typically increase the  $p\text{CO}_2$  of a soil through direct and indirect processes. However, most authors have concluded that the overall effects of these chemical factors will be less than a factor of 10 in the weathering rate (e.g. Drever 1994).

Plants have an additional effect on physical factors in the weathering environment: plants bind fine particles to the soil, thus increasing the surface area exposed to soil porewaters. They also increase the residence time of water in soil systems, increase evapotranspiration, and increase permeability in some soils. Drever (1994) concludes that, in regimes with thin soils where mineral dissolution limits weathering, plants increase the weathering rate as a result of increased contact time and surface area. In contrast, in regimes where mechanical erosion limits weathering fluxes, the precipitation of secondary phases and the development of a deep regolith (both of which are encouraged by plants) will decrease or leave unchanged the chemical weathering rates.

## CONTROLS ON CHEMICAL EROSION

Chemical erosion is the process whereby the dissolved products from chemical weathering are transported from the weathering environment to sites of eventual precipitation and removal with sediments. It is quantified as the product of stream concentration and discharge. In this sense it is distinguished from chemical weathering (the process of mineral dissolution in the soil environment), though the terms are often used interchangeably. The framework for considering the controls on chemical erosion at the watershed to global scale was established by Stallard & Edmond in a series of classic papers on the Amazon drainage basin (Stallard & Edmond 1981, 1983, 1987; Stallard 1985). They taught us that traditional indicators of rapid chemical weathering, e.g. thick, cation-depleted soils, were instead indicative of just the opposite: very low rates of chemical weathering at present. The potential for chemical weathering in tropical climes is high because soils remain warm and wet; however, the establishment of a thick soil mantle in

environments undergoing little physical disturbance prevents the interaction between soil waters and fresh bedrock. As a result, the bulk of the chemical load in the Amazon is derived not from such regions low in the Amazon basin, but rather from high in the Andes where soils are thin and immature. Stallard & Edmond identified two end-member states for the controls on chemical erosion: the so-called transport-limited and weathering-limited erosional regimes.

## Weathering and Transport Limitation

Transport-limited watersheds have thick, mature soils in which most of the primary minerals (e.g. feldspar, hornblende, and mica) have been altered to secondary minerals, depleted in soluble cations ( $\text{Ca}^{2+}$ ,  $\text{Mg}^{2+}$ ,  $\text{Na}^+$ ,  $\text{K}^+$ ). Hydrologically important flowpaths travel through this cation-depleted soil without interacting with bedrock, so the streams are especially dilute. In these cases, the flux of dissolved ions is limited by the inability of these systems to erode the soil mantle and bring fresh, unaltered minerals in contact with through-flowing soil waters.

In contrast, soils in high-relief regions are thin. Rainwater percolates readily to the bedrock-soil interface, where it interacts with fresh minerals. Water and soil residence times are short, so the minerals more susceptible to dissolution come to dominate the stream chemistry.

Overall, transport-limited streams tend to be characterized by low rates of chemical erosion, limited by the rate of physical erosion of the soil mantle (which itself may be limited by slow or negative rates of surface uplift). Chemical erosion in weathering-limited regions, on the other hand, is rapid and limited by the factors that control mineral dissolution rates, including mineralogy, water supply (net precipitation), soil-water pH, and temperature.

## Clues from Ge/Si Ratios

An important question is raised in this context: Is the global chemical erosion rate weathering-limited or transport-limited? One approach to answering this question is to consider the relative concentrations of germanium (Ge) and silicon (Si) in the world's rivers. Ge and Si have very similar but not identical geochemical behaviors, and thus have been used in the same way as isotopic ratios to elucidate geochemical processes (e.g. Froelich et al 1985, Mortlock & Froelich 1987, Murnane & Stallard 1990). During incongruent silicate mineral dissolution, which is characteristic of weathering-limited regions, Ge is preferentially incorporated into secondary soil minerals (clays). Streams draining such regions therefore tend to have Ge/Si ratios smaller than those of the primary minerals being dissolved. The more complete dissolution of primary minerals in transport-limited regions, coupled with the dissolution of Ge-rich secondary clays transported from the upper, weathering-limited part of the watershed, leads to Ge/Si ratios that can equal or even exceed that of the primary minerals. Therefore, the Ge/Si ratio of rivers is a fair indicator of the relative importance of weathering versus transport limitation.



The transport-limited regions of the Amazon basin have Ge/Si ratios of approximately  $1.7 \times 10^{-6}$ , whereas the weathering-limited streams of the Andes have Ge/Si ratios as low as  $0.42 \times 10^{-6}$ . If we compare these end-member ratios to the globally averaged river ratio provided by Mortlock & Froelich (1987) of  $0.6 \times 10^{-6}$ , we see that chemical erosion by the world's rivers is strongly weathering-limited.

## Temperature Versus Rainfall as Controls on Chemical Erosion

The conclusion that chemical erosion at the global scale is weathering-limited has important implications for our discussion of what controls atmospheric  $p\text{CO}_2$  and climate. What this means is that the factors that control soil mineral dissolution (temperature, rainfall, soil solution pH, mineralogy, mineral surface area, and chelate concentration) are what control global  $\text{CO}_2$  consumption rates—not the rate of uplift and soil erosion. This assertion is in stark contrast to the position of Edmond and colleagues (e.g. Edmond et al 1995, Huh & Edmond 1999, Edmond & Huh 1997), who have argued repeatedly for the premier importance of tectonics. Clearly, chemical erosion rates would increase if regions presently categorized as transport-limited were subjected to uplift and physical erosion, but this would simply make the world, as a whole, more weathering-limited.

**Precipitation/Runoff** Presuming that there are climatologic controls on global weathering, we would still like to know whether net precipitation or temperature is the more important climatic variable. A critical observation in this regard is that the chemical flux of dissolved material for most rock-derived elements and for most rivers increases with discharge, because concentration doesn't follow a simple dilution trend with increasing flow (Holland 1978, Bluth & Kump 1994; Figure 6). This indicates that increases in water delivery to most large watersheds do not result in simple dilution; watershed chemical yield increases with discharge, but the increase is logarithmic (some dilution occurs). Ultimately, at very high discharge, the maximum yield of a watershed is reached, and further increases lead to simple dilution.

A more detailed look at river compositional and hydrological data compiled for basalt catchments from around the world (Bluth 1990, Bluth & Kump 1994) reveals some interesting consistencies that we do not yet fully understand (Figure 8, Table 4). Each of the major dissolved constituents (K, Na, Ca, Mg,  $\text{HCO}_3$ , total dissolved solids, and  $\text{SO}_4$ ) displays a plateau concentration at low runoff, a break to the data in this upper envelope at a runoff value of around 1 cm/yr, and a region of dilution at higher runoff values (up to  $\sim 1,000$  cm/y) in which the upper envelope slopes downward with a slope of  $-0.5$  in log-log terms. Silica behaves somewhat differently (Table 4); its breakpoint appears to be at a slightly higher runoff ( $\sim 3$  cm/y), and its dilutional slope is also considerably shallower than that of the other species ( $-0.1$  in log-log terms).

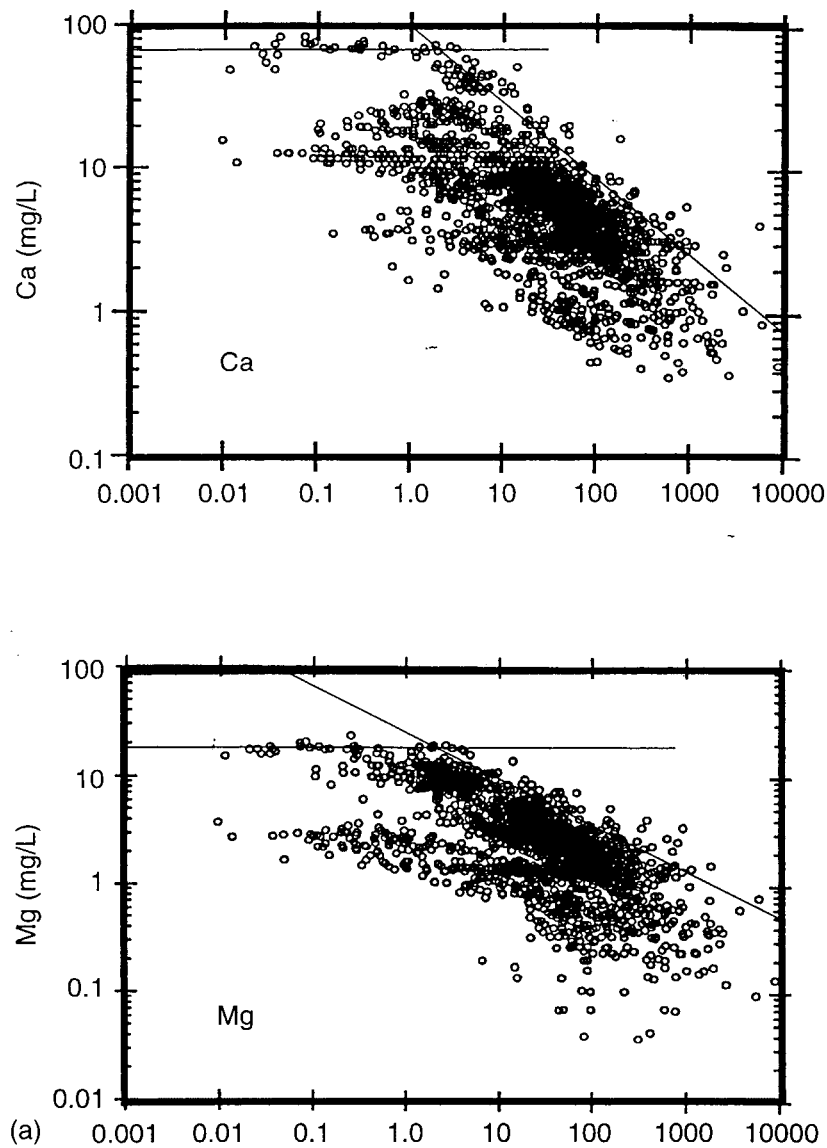


**Figure 8** Concentration-discharge relationships for monolithic basalt catchments of the world. Data are shown for Ca, Mg, K, Na,  $\text{SO}_4$ , and total dissolved solids (TDS). Source of data is Bluth (1990).

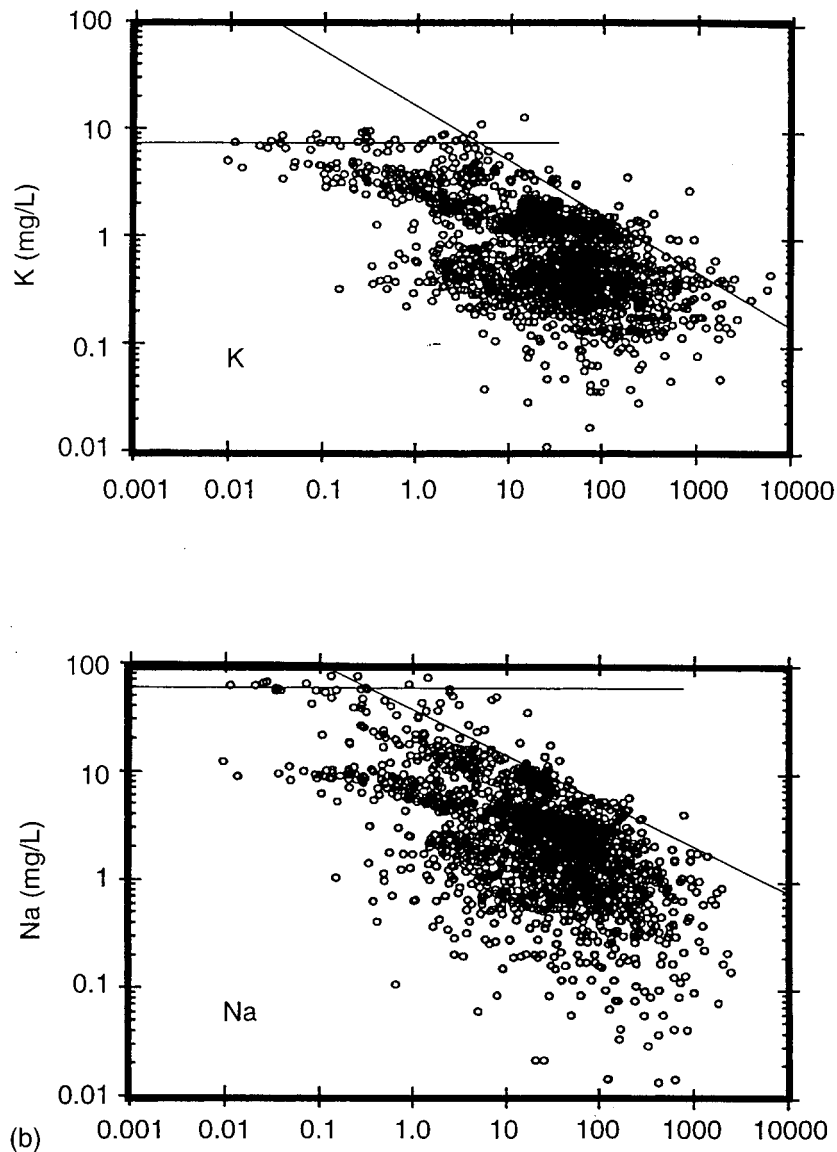


**Figure 8** Concentration-discharge relationships for monolithologic basalt catchments of the world. Data are shown for Ca, Mg, K, Na,  $\text{SO}_4$ , and total dissolved solids (TDS). Source of data is Bluth (1990).

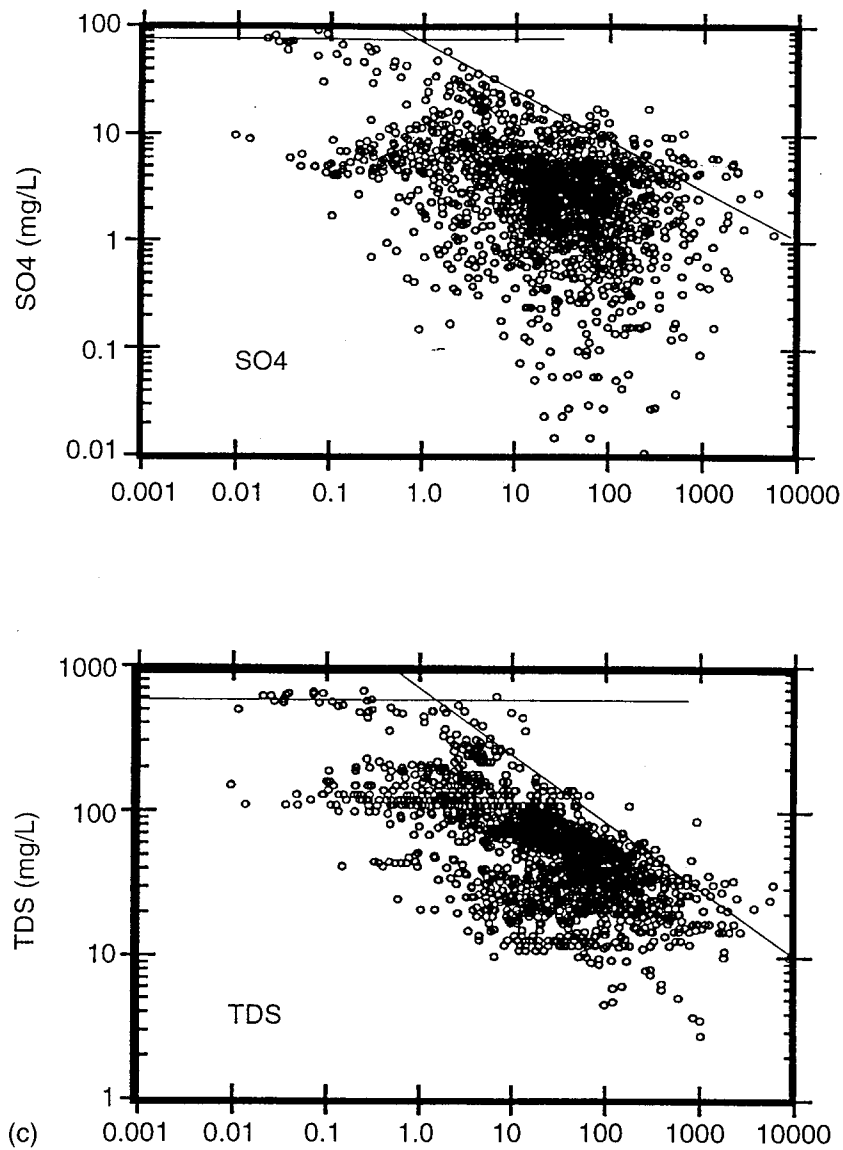


**Figure 8** Concentration-discharge relationships for monolithic basalt catchments of the world. Data are shown for Ca, Mg, K, Na, SO<sub>4</sub>, and total dissolved solids (TDS). Source of data is Bluth (1990).

**TABLE 4** Characteristics of concentration/runoff relationships for basalt catchments (refer to Figure 8; after Bluth 1990).

Element	Plateau concentration (ppm)	Plateau breakpoint (cm/y)	Slope beyond breakpoint ( $\Delta \log C^a / \Delta \log R^b$ )
K	10	1	-0.5
Na	60	1	-0.5
Ca	70	1	-0.5
Mg	20	1	-0.5
HCO <sub>3</sub>	200	1	-0.5
TDS <sup>c</sup>	600	1	-0.5
SO <sub>4</sub>	80	1	-0.5
SiO <sub>2</sub>	40	3	-0.1

a. concentration (ppm)

b. runoff (cm/y)

c. total dissolved solids (ppm)

The plateau concentrations for bicarbonate and silica may represent saturation of river waters with calcite and moganite (a silica polymorph), respectively (Heaney & Post 1992, Gislason et al 1996, Gislason & Arnorsson 1993, Bluth & Kump 1994). The plateau concentrations for K, Na, and Mg may also represent saturation with secondary phases under the low-flow conditions represented by runoff values of less than 1 cm/y (Gibbs 1970, Garrels & Mackenzie 1967).

The dilutional slope of -0.5 (log-log) for all species except silica means that their concentration decreases with the square root of the runoff. We can proffer no elegant explanation for the slope of this relationship. It does indicate that some buffering of concentration occurs, perhaps by ion exchange in soils, as the supply of water to the weathering environment increases. An important role for ion exchange in soils, insofar as regulating river composition and elemental flux, has been indicated by the relationships among the dissolved constituents in streams (Drever 1988, Bluth & Kump 1994) and implicated as a buffering mechanism for soil waters (Gwiazda & Broecker 1994, Berner et al 1998). Another explanation for the shallow dilutional trend for silica is that dissolution rates of primary minerals increase or precipitation rates of secondary minerals decrease as net precipitation (and ultimately runoff) increases, because soil waters become more undersaturated with respect to these phases (e.g. Gislason et al 1996). The shallow dilutional trend for silica may then reflect faster dissolution of secondary or biogenic silica phases under wet conditions.

**Temperature** The dependence of elemental flux on temperature has been more difficult to demonstrate. The fundamental problem with attempts to extract a temperature dependence from field data at the watershed scale is the co-dependence of other factors that affect weathering with mean temperature—

namely, precipitation and evaporation, vegetation cover, and the extent of prior soil development and cation leaching. Such factors can dominate chemical erosion, and in many cases may act to reduce rather than accelerate it. For example, Icelandic streams exhibit higher chemical erosion rates at a given stream discharge than do Hawaiian streams (Bluth & Kump 1994). At some point in the past, these Hawaiian streams were probably yielding a higher chemical load as the soils were developing. Now, however, the soils are highly leached and unable to support high chemical yields. In contrast, Icelandic soils are relatively immature, and weathering may be enhanced by the presence of fractured basalt (Berner & Berner 1997).

Despite these problems, indications that temperature plays a role in determining rates of chemical erosion do exist. For example, Meybeck (1980) found that the Si concentration of streams increases with the annual average temperature of some French watersheds. Presuming that these results are not simply the result of concentration via evaporation (White & Blum 1995) or dilution due to higher discharge in the cooler environments (no discharge data were given), this increase in concentration with temperature supports a temperature feedback. However, Meybeck's observations have been alternatively interpreted as the result of the tendency for silica-rich clays to form in the cooler watersheds, which reduces the supply of silica to streams, and of the tendency for silica-poor clays to form in warmer regions, which increases the dissolved silica concentrations in streams draining them (Berner & Berner 1996).

Velbel (1993) used a clever approach to isolate the effects of temperature on weathering in a study of watersheds draining the Blue Ridge Mountains of the eastern United States. Two adjacent watersheds were chosen for their lithological and climatic similarity but their differing mean elevation—one centered at 849 m and the other at 1019 m above sea level. Velbel (1993) found that the lower elevation watershed had a larger chemical yield, which he attributed to the slightly warmer mean annual temperature of that watershed (11.7°C vs. 10.6°C). In conjunction with these temperature estimates, he was able to calculate an activation energy for the weathering reactions (18.4 kcal/mol) that was significantly higher than those determined in laboratory experiments; this suggested a strong temperature feedback on chemical erosion.

There are some reasons why this study in itself should be considered suggestive, rather than conclusive, in terms of a field demonstration of a temperature effect. The two watersheds, though differing in mean elevation, overlapped in their range of elevations; it is unknown where in these watersheds the bulk of weathering was occurring. Moreover, estimated atmospheric lapse rates, rather than actual climatological data, had to be used to estimate average temperatures. Soils in these areas are thick (averaging 6 m), which indicates that these catchments are not typical of weathering-limited regimes where temperature dependence is predicted. Therefore, the results need to be confirmed by other similar studies.

Berner et al (1998) argue that seasonal fluctuations in major ion and silica concentrations in soil waters draining experimental plots in the Hubbard Brook, New Hampshire watershed result from seasonal temperature cycles—which modulate ion-exchange equilibria and biogenic acid production—rather than from fluctuations in water discharge. Soil waters apparently reach ion-exchange equilibrium quickly (on the time scale of individual rain events), so that the tendency for dilution under high flow (or concentration during periods of net evapotranspiration) is obscured. Because stream waters commonly exhibit dilutional responses to increased flow (e.g. Miller & Drever 1977, Richards 1999), hydrological factors may become more important at the larger scale of natural watersheds.

The relationship between elevation and chemical weathering has the potential to reveal a temperature effect, although other factors that correlate with elevation—including relief, rainfall, soil thickness, and vegetation cover—emerge as important determinants. Elevation itself has no direct effect on chemical weathering. Drever & Zobrist (1992) reported a strong trend in chemical erosion with elevation in a study conducted in the Swiss Alps. These granitic gneiss catchments had similar slopes and soil mineralogies, but differed in mean elevation (from 360 m to 2,400 m); annual average temperature (no values given); vegetation coverage (from deciduous forest at low elevation, through coniferous forest and alpine pasture, to bare rock and talus at the highest elevations); soil thicknesses that decreased from about 1.5 m at low elevations to zero at high elevations; and precipitation (ranging from 1.9 m/y–2.4 m/y; elevation trend not given). These differences conspired to cause an exponential decrease in chemical yield (e.g. based on alkalinity fluxes) with elevation. The authors ascribed most of the twenty-fold decrease in alkalinity yield to longer residence times for soil waters in the lower elevations; soils act as a sponge for precipitation, increasing moisture availability for mineral dissolution. Apparently, the rate of mineral dissolution is limiting the flux at higher elevations because through-flowing waters have little time to interact with soil minerals. This indication of weathering limitation is consistent with the authors' interpretation based on the fact that soils are thin throughout the study area. Berner (1994) interprets these data in a somewhat different fashion, concluding that vegetation cover is an equally important factor, perhaps responsible for as much as a seven-fold increase in chemical erosion rate.

In contrast, an increase in soil development and leaching with elevation has been documented for the Sierra Nevada mountains of California (Dahlgren et al 1997). Here, rainfall amounts correlated with elevation. Higher precipitation at higher elevation creates a more leached soil dominated by aluminum and iron oxides. At lower elevations, more cation-rich soil minerals are present. No stream data are available from this study to assess whether the maturity of the soil affects the riverine flux of the elements.

Given that the extent of soil development may be obscuring the temperature effect, there are two ways to proceed. One is to study only weathering on bare rock, and the other is to try to isolate the temperature effect using multivariate

approaches. Two recent studies exemplify both approaches. The first approach was taken by Dorn & Brady (1995), who confined their analysis to the uppermost soil- and lichen-free surfaces of basalt exposures along an elevational transect in Hawaii. Moreover, they removed the effects of variable rainfall by sampling weathering rinds along the 500 mm/yr isohyet from four different elevations ranging in mean annual temperature from 12.5 to 23.3°C. By quantifying the extent of mineral dissolution (units of % weathered per thousand years) using back-scattered electron microscopy, they were able to determine an activation energy for chemical weathering of plagioclase of 26.2 kcal/mol. This value is somewhat higher than Velbel's (1993) field-based value of 18.4 kcal/mol, or various laboratory determinations (ranging from 15–22 kcal/mol; see earlier section entitled Mineral Dissolution in the Laboratory and Field).

In perhaps the most rigorous attempt to date to eliminate all variables except temperature from a multivariate dataset, White & Blum (1995) compiled data on watersheds from around the world, focusing on those dominated by granitic terrains. Their watersheds spanned temperate to tropical climates, though all but four were in North America and Europe. Although there was the inevitable scatter in the data, the tropical watershed (Rio Icacos, Puerto Rico) clearly exhibited higher rates of chemical erosion. White & Blum (1995) fit an Arrhenius-type equation to data on silica and sodium fluxes, and calculated an activation energy that was consistent with laboratory data on feldspar dissolution. Ca, Mg, and K weathering fluxes did not correlate with temperature, which suggests that other factors control their release to streams. White & Blum (1995) developed a function that predicted riverine flux of Na and Si as a linear function of precipitation and an Arrhenius-type temperature dependence; this function was able to fit the data well. The activation energy they determined was about 15 kcal/mol, which is consistent with laboratory determinations we cited previously. However, we must point out that the high correlation coefficient ( $r^2 = 0.91$  for  $\text{SiO}_2$  and 0.83 for Na) is strongly dependent on the data from Rio Icacos. More studies of tropical watersheds are clearly needed.

## MODELS OF CHEMICAL WEATHERING AND EROSION

So far we have explored the connection between climate variables and weathering rate. In theory, however, weathering also provides a negative feedback to climate on the long term (Walker et al 1981). Because atmospheric carbon dioxide concentration is expected to have been the primary control on global climate, at least during the Phanerozoic (e.g. Berner 1998), the consumption of carbon dioxide during weathering therefore helps regulate  $p\text{CO}_2$ .

Models of the role of weathering on the global carbon cycle have traditionally separated the organic carbon cycle from the inorganic carbon cycle or the carbonate-silicate cycle. The long-term organic carbon cycle involves the burial in sedimentary basins of the small fraction of photosynthesized organic carbon



that survives decomposition in soils, ocean waters, and marine sediments, as well as its weathering upon exposure in terrestrial environments undergoing exhumation and erosion. The carbonate-silicate cycle, on the other hand, involves the consumption of atmospheric CO<sub>2</sub> during the weathering of silicate rocks, which is thought to be balanced on long time scales by the release of CO<sub>2</sub> from volcanoes and metamorphic zones.

### Mass Balance in the Modern Carbonate-Silicate Cycle

The riverine alkalinity flux directly reflects the consumption of atmospheric CO<sub>2</sub> during chemical weathering. The fraction of this flux originating from silicate weathering represents a long-term sink for atmospheric CO<sub>2</sub> that is balanced by the net release of CO<sub>2</sub> from volcanism and metamorphism, and from the excess of oxidative weathering of organic carbon over deposition. Generally, it is thought that deposition of organic carbon is equivalent to the oxidation flux; however, periodic imbalances in the organic-carbon subcycle are potentially large, and can be estimated using the carbon isotopic record (Lasaga et al 1985, Berner 1994, Kump & Arthur 1997). Nevertheless, much of the modeling that has been done to date has focused on the carbonate-silicate cycle, rather than the organic-carbon cycle, partly because the identification of negative feedbacks in the organic carbon cycle has been an elusive goal (c.f. France-Lanord & Derry 1997, Raymo 1997, Follmi 1995, Delaney & Fillippelli 1994, Worsley et al 1988). Because this is to be a review with extensions of recent work, our primary focus is on the carbonate-silicate cycle.

There has been considerable interest in assessing the mass balance in the modern carbon cycle, and some estimates have included the long-term carbonate-silicate cycle. Typical estimates of the annual amount of carbon consumed during silicate weathering range between 6 and 6.6 Tmol y<sup>-1</sup>. If we take the reasonable median estimates of present-day CO<sub>2</sub> degassing associated with subaerial (ca. 1.5 Tmol y<sup>-1</sup>) and submarine (ca. 2.5 Tmol y<sup>-1</sup>) volcanism, we find that the flux is about two-thirds of that needed to balance the carbon cycle (Varekamp et al 1992, Arthur 1999). However, it has also been suggested that alteration of oceanic crust represents an additional carbon sink of 2–3 Tmol y<sup>-1</sup> over that required for subaerial weathering (Staudigal et al 1989). Estimates for the ocean crustal alteration carbon sink have been raised subsequently to 3.7 Tmol y<sup>-1</sup> (Varekamp et al 1992). If the latter estimate is valid, the basalt alteration source would demand all of the estimated midocean ridge carbon flux and more, and would increase the total CO<sub>2</sub> outgassing flux required to balance the carbon cycle to about 10 Tmol y<sup>-1</sup>. In other words, the metamorphic-hydrothermal flux would have to be 6 Tmol y<sup>-1</sup>, assuming a total volcanic flux of 4 Tmol y<sup>-1</sup> given above. These fluxes are nearly the same as the estimated amounts of organic carbon oxidized and deposited annually (10 Tmol y<sup>-1</sup>). These uncertainties mean that we cannot conclusively determine whether the modern-day carbonate-silicate cycle is balanced. On the other hand, the fluxes yield a response time that is on the order of 10<sup>5</sup> y for the

ocean-atmosphere carbon reservoir, much longer than is of concern to a society coping with the consequences of fossil-fuel burning. However, small imbalances with respect to the uncertainty of these estimates can generate large excursions in atmospheric  $p\text{CO}_2$  if they persist for hundreds of millennia or longer. We will explore this possibility in the final section of this paper.

## Globally Averaged Box Models

Although a number of numerical modeling experiments of varying complexity have been performed on the carbonate-silicate cycle, the gist of the approach is well expressed by an equation presented by Edmond et al (1995):

$$\frac{d}{dt} p\text{CO}_2 = \emptyset - (k \cdot A_{\text{ex}} \cdot p\text{CO}_2) \quad (15)$$

where  $\emptyset$  is the flux of  $\text{CO}_2$  from volcanoes and metamorphic zones,  $k$  is a rate constant, and  $A_{\text{ex}}$  is the effective area of exposure of fresh minerals (relative to today). This equation states that the rate of change of atmospheric  $p\text{CO}_2$  is determined by the magnitude of the imbalance between the rate of addition of  $\text{CO}_2$  to the atmosphere through volcanism/metamorphism and the rate of removal through weathering. Moreover, it states that the rate of weathering is functionally dependent on the amount of fresh silicate mineral surface available for weathering *and on atmospheric  $p\text{CO}_2$* . If atmospheric  $p\text{CO}_2$  rises, the weathering rate increases; if it goes down, the weathering rate decreases. This creates a negative feedback loop (Figure 1) that is potentially capable of stabilizing atmospheric  $p\text{CO}_2$  on long time scales.

A debate has been raging about the efficacy of this climate weathering feedback; the main proponent is Robert Berner of Yale University, and the main opponent is John Edmond of the Massachusetts Institute of Technology. Edmond et al (1995) used Equation 15 in an argument for the paramount importance of tectonics, as reflected in the term  $A_{\text{ex}}$ , in the regulation of atmospheric  $p\text{CO}_2$ . Uplift generates relief, which facilitates the removal of the cation-depleted soil mantle; this enhances the interaction between surface waters and primary minerals. They claim that this reasoning contrasts with that of Walker et al (1981) and Berner et al (1983), which focuses “on the level of atmospheric  $\text{CO}_2$  as the driving agent of chemical weathering” (Edmond et al 1995). However, their formulation (Equation 15) does state that the weathering rate is linearly dependent on atmospheric  $p\text{CO}_2$ , which is a considerably stronger sensitivity than the logarithmic relationship proposed by Walker et al (1981) or Berner et al (1983).

Edmond et al (1995) do not elaborate on the mechanism they envision that links weathering to atmospheric  $p\text{CO}_2$ , and whether it is direct or indirect. The initial Walker et al (1981) treatment used early laboratory experiments of the direct effects of  $\text{CO}_2$  in accelerating weathering to parameterize the weathering flux. In more recent experiments cited in the previous section, increased  $p\text{CO}_2$

has been shown to affect (decrease) dissolution of some Mg- and Ca-containing silicates only at high pH. Berner et al (1983) recognized that the major effect of CO<sub>2</sub> on weathering was probably indirect, and involved the greenhouse effect of atmospheric *p*CO<sub>2</sub> on temperature and net precipitation. Part of the argument for an indirect effect is the observation that soil atmospheres tend to have partial pressures of CO<sub>2</sub> that are 10–100 times the atmospheric value (Amundson & Davidson 1990) as a result of root respiration and microbial decomposition. Thus, the *p*CO<sub>2</sub> of the weathering environment is determined by soil biological activity, not by atmospheric *p*CO<sub>2</sub>. However, atmospheric *p*CO<sub>2</sub> can affect soil biological activity, through its direct effect on plant productivity (Volk 1987, Kump & Volk 1991, Berner 1994, van der Sluijs et al 1996) and its indirect effect on temperature and moisture availability. Any connection between CO<sub>2</sub> and weathering must therefore be indirect. Whatever the nature of the relationship, the key point is that for steady state to be established, weathering rates must be sensitive to atmospheric *p*CO<sub>2</sub>.

The importance of tectonics as a forcing factor was taken up by Berner in his later modeling (Berner 1994). Thus, despite arguments to the contrary (Edmond & Huh 1997, Berner & Caldeira 1997), the two schools of thought are in fact one: tectonic factors such as volcanism, uplift, and exposure affect atmospheric *p*CO<sub>2</sub>, but ultimately the stabilizing influence is the sensitivity of weathering rates to atmospheric *p*CO<sub>2</sub>. Increases in relief in tectonically active regions of the world increase *A<sub>ex</sub>*, and thus cause CO<sub>2</sub> draw-downs. The attendant climate change reduces chemical weathering rates elsewhere, returning the carbonate-silicate cycle to steady state (Kump & Arthur 1997).

## Geographically Resolved Models

The models discussed so far are zero-dimensional in that their state variables are global averages. Very few attempts have been made to resolve spatial variations in chemical erosion and CO<sub>2</sub> consumption rates—and thus the geographical complexity of the weathering-climate connection—either for the present day or the geological past. To do so requires additional information on the geographic distribution of the types of rocks undergoing weathering (Bluth 1990, Bluth & Kump 1991) and of the factors that influence chemical weathering and erosion (Bluth 1990).

Probst and colleagues have been developing techniques for assessing weathering-associated CO<sub>2</sub> consumption rates for specific basins for which lithological distributions can be estimated (Amiotte-Suchet & Probst 1993, Probst et al 1994, Ludwig et al 1996, Boeglin & Probst 1998). This involves establishing empirical relationships between riverine alkalinity flux and the temperature, runoff, and lithology of watersheds, a task also undertaken by Bluth & Kump (1994). The empirical relationships seem to work quite well in a predictive mode. For example, Gaillardet et al (1995) found that empirical relationships from Bluth & Kump

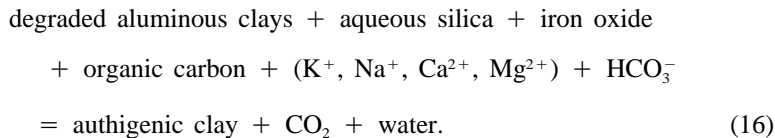
(1994) were accurate predictors of bicarbonate and silica yield from the Congo river basin.

These groups extended their approach to the global scale, and the results have demonstrated the importance of adding a spatial dimension to global geochemical models. Gibbs & Kump (1994) and Ludwig et al (1998) have used flux-runoff relationships and various sources of climatological and lithological data to estimate chemical erosional fluxes for the world's rivers, both for the present day and the last glacial maximum (21–18 k.y.). On the Quaternary time frame, the potentially conspiratorial effects of changes in climate and exposure are not well realized. However, Gibbs & Kump (1994) did find that the potential reduction in chemical erosion under glacial maximum conditions—as a result of ice-sheet coverage of much of North America and northern Europe and a general reduction in Northern Hemisphere runoff—was offset by exposure via sea-level fall in lower latitudes of less resistant carbonate lithologies. Sloan et al (1997) used global climate model output and the lithological maps of Bluth & Kump (1991) to simulate the spatial distribution of Eocene weathering rates. Although the climate model results suggested that Eocene river discharge was enhanced, chemical erosion rates were lower than they are today because of a smaller area of exposure of more easily weathered lithologies. Most recently, Gibbs et al (1999) have used this approach to study chemical erosion rates from the Triassic to the Recent, using output from an atmospheric general circulation model run for a suite of paleocontinental configurations and atmospheric  $p\text{CO}_2$  levels. They find that the largest determinant of secular changes in chemical erosion is changes in global runoff brought about by continental drift. The Triassic, a time of supercontinent assembly, was arid and dominated by internal drainage, and exhibited the lowest chemical erosion rates; however, the opposite was found for the later Mesozoic, a time of continental dispersal. This comparison holds for a variety of specified atmospheric  $\text{CO}_2$  concentrations, which suggests that continental size and position are the major determinants of the intensity of the continental hydrological cycle. This relationship between continentality and runoff is well known, and has been used in predictions of paleorunoff in the past (Tardy et al 1989). It suggests, however, that the balance between global silicate weathering ( $\text{CO}_2$  consumption) and  $\text{CO}_2$  release by volcanism may be achieved in part through their common dependence on the Wilson cycle of continental assembly and dispersal (Gibbs et al 1999).

A significant difference between the geographically resolved models and the global models is that the former calculate weathering rates as functions of prescribed climates (either the modern observed climate or paleoclimates modeled using global climate models), whereas in the globally averaged models, global climates and weathering rates are solved simultaneously and co-evolve in response to external forcings. Such coupling is presently not feasible for the geographically resolved models.

## THE GEOLOGIC RECORD OF CLIMATE—WEATHERING FEEDBACK

Because the size of the ocean-atmosphere carbon dioxide reservoir today is about  $3.8 \times 10^6$  Tmol, one would expect that a relatively small ( $<1$  Tmol  $y^{-1}$ ) imbalance in either the outgassing/weathering or organic-carbon oxidation/deposition subcycles would, on a scale of  $10^6$  years, produce substantial changes in atmospheric  $p\text{CO}_2$ . Thus, if major changes in volcanic-metamorphic outgassing have occurred in the past, we expect that the weathering feedback would certainly have operated in order to prevent major excursions in  $p\text{CO}_2$  and climate from occurring (Berner & Caldeira 1997). An interesting alternative to the climate-weathering feedback is the putative reverse weathering buffer, i.e. the equilibration of the ocean with K, Na, Mg, and Ca-rich silicate minerals formed during early diagenesis. Reverse weathering has been proposed as a buffer for seawater composition, including its pH and alkalinity (Sillen 1961, Mackenzie & Garrels 1966). As McCauley & DePaolo (1997) point out, although it was popular in the 1960s and 1970s, this equilibrium concept was abandoned in favor of the dynamic model of seawater composition typified by the Berner et al (1983) BLAG model. This happened for various reasons, including the fact that widespread authigenic, cation-rich clays were not to be found. Interest in reverse weathering has been renewed following the work by Michalopoulos & Aller's (1995) work on the Amazon delta sediments (Mackenzie & Kump 1995, McCauley & DePaolo 1997). A schematic of the reverse weathering process is as follows (Mackenzie & Kump 1995):



If the ocean is indeed buffered with vast amounts of authigenic clays, then substantial imbalance in the carbon cycle could be compensated for by adjustments in the cation-content of the clays. For example, an interval of intense volcanism and release of  $\text{CO}_2$  would release cations from authigenic clays back into solution, converting aqueous  $\text{CO}_2$  to  $\text{HCO}_3^-$  and thus providing a sink for the volcanic  $\text{CO}_2$ . McCauley & DePaolo (1997) estimate this buffer as being six times larger than the carbonate system in the oceans. Thus, it could accommodate significant imbalances in the carbon cycle for periods of up to millions of years rather than hundreds of thousands of years—though it is unclear whether it has the capacity to offset the effects of 40 million years of Himalayan mountain building. Moreover, the overall reaction for silicate weathering/reverse weathering is much like that for carbonate weathering, in that it provides no net sink for  $\text{CO}_2$  on the long term.  $\text{CO}_2$  is consumed in the weathering of primary minerals, and in the process, bicarbonate and dissolved cations are released to soil solutions and quickly trans-

ported to the ocean. On time scales ranging from similarly short periods to many millions of years later, the degraded solid products (clays) are eroded and transported to the ocean, where reverse weathering potentially takes place. Reacting with silica, iron oxides, organic matter, soluble cations, and bicarbonate, these degraded clays are transformed into cation-rich clays, and in the process carbon dioxide is released. Thus, on the time scale of soil residence times (millennia to millions of years) there is no net effect of silicate weathering and reverse weathering on the alkalinity and CO<sub>2</sub> balance of the ocean-atmosphere system.

Although Earth's climate has alternated on longer time scales during the Phanerozoic between greenhouse and icehouse climates (e.g. Fischer 1982), the lack of evidence for runaway climatic states suggests that the climate-weathering feedback is effective overall (e.g. Berner & Caldeira 1997, Berner 1998). Nonetheless, variations in continental area, continental distribution with respect to climatic zones, exposure of silicate rocks with respect to other rock types, relative importance of tectonic uplift and average soil thickness,  $p\text{CO}_2$ , and global climate regime are all factors that must be considered as possibly impacting the effectiveness of weathering over geologic time. These and other events such as the timing of the rise and spread of vascular plants are all factors that may have induced significant variations in the susceptibility of the land surface to chemical erosion (its weatherability). In the next section, we explore a few examples of both effective and ineffective weathering-climate feedback in the geologic record.

### How Would We Detect Variations in Weathering Intensity in the Geologic Record?

Most of the possible geochemical proxy indicators of weathering intensity on the continents are monitors of changing ocean chemistry that leave a sedimentary record. These include variations in radiogenic isotope ratios ( $^{87/86}\text{Sr}$ ,  $^{143/144}\text{Nd}$ ,  $^{187/186}\text{Os}$ ) recorded by carbonate and phosphate minerals precipitated from seawater, global carbonate burial rate variations, variations in global opal/chert deposition, and elemental ratios such as Ge/Si. All of these reflect either changes in fluxes of dissolved species delivered by rivers or changes in mean composition of riverine dissolved components. However, these are not infallible indicators of changing weathering fluxes; this is because of the assumptions that must be made when interpreting them, not to mention the difficulty in locating pristine, unaltered samples for analysis.

Many of the elemental and isotopic ratios recorded by minerals precipitated from seawater represent a mean of two or more inputs. For example, the strontium isotope mass balance for seawater must take into account the more radiogenic strontium supplied by rivers—which represents weathering of rocks with widely varying strontium isotope signatures—and the isotopic imprint of hydrothermal exchange of strontium at mid-ocean ridges. Although the isotopic composition of the hydrothermal strontium is probably reasonably constant through time because of the relative constancy of the  $^{87/86}\text{Sr}$  in mid-ocean ridge basalts, the hydrother-

mal Sr flux to seawater almost certainly is not constant. Any interpretation of changing Sr isotope ratios in seawater through time (Figure 9) must take into account possible variations in this flux. Most quantitative models of the Sr isotope record (e.g. Kump & Arthur 1997) assume that the hydrothermal flux is scaled linearly with rates of ocean crust production. Although such an assumption is not unreasonable, we simply do not know how the flux would vary with changing

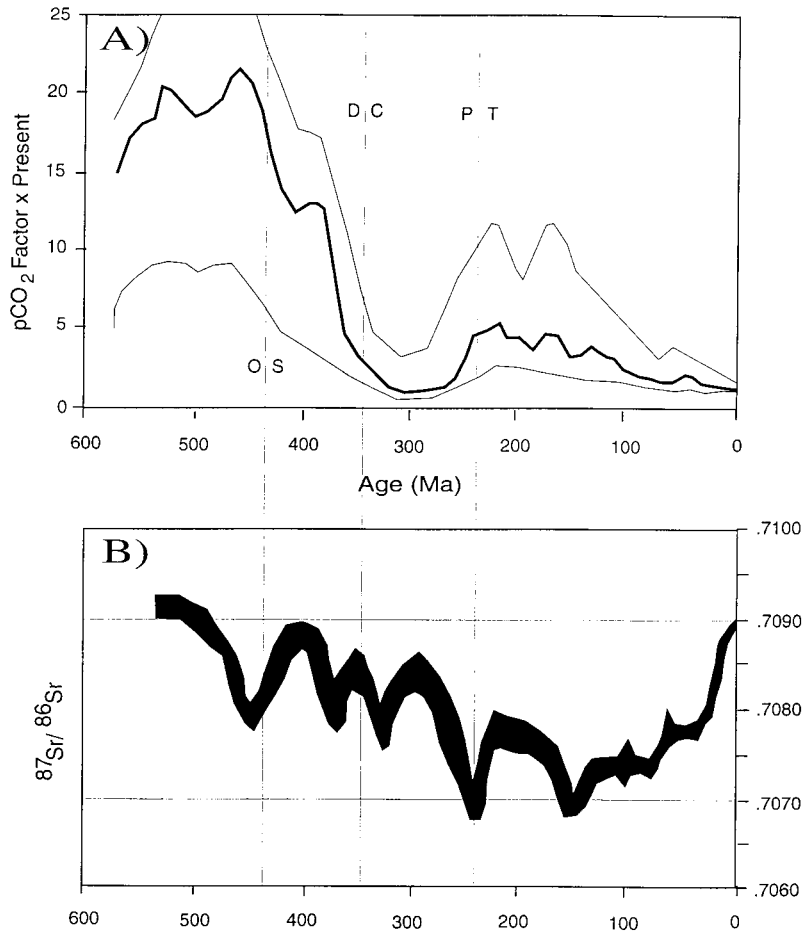


**Figure 9** (A) Possible history of atmospheric carbon dioxide concentrations ( $p\text{CO}_2$  relative to the present) for the Phanerozoic from the GEOCARB II model of Berner (1994). The dark curve is Berner's preferred scenario, whereas the bounding curves represent the range of estimates based on different boundary conditions for simulations. (B) A strontium isotope curve for marine carbonates (after Denison et al 1998). The width of the curve represents an estimate of the uncertainty in determining the  $^{87}/^{86}\text{Sr}$  ratio from available data.

crustal production. In addition, there is no way to know the history of rates of oceanic crustal production in detail beyond about 150 Ma, because of the progressive destruction of older seafloor by subduction. Nonetheless, one might attempt to constrain hydrothermal contributions using Li/Ca ratios in carbonates (e.g. Delaney & Boyle 1986).

With respect to weathering, changing seawater Sr isotope values could reflect either increasing flux of riverine strontium of constant Sr isotopic ratio, or a change in the mean Sr isotopic ratio of riverine Sr. In this regard, few studies of seawater Sr isotope variation have considered that the Sr isotopic composition of what was weathered changed, as opposed to a changing Sr flux from weathering. For example, the rapid increase in the seawater  $^{87/86}\text{Sr}$  ratio in the Neogene (Figure 9) led Raymo et al (1988) to posit a relationship between uplift of the Himalayas (see discussion later in this section) and an increase in weathering rate and climatic cooling. However, subsequent workers have argued that the increase in seawater  $^{87/86}\text{Sr}$  is a source signal rather than a global increase in radiogenic Sr from weathering (e.g. Edmond 1992). Recent Sr isotope data for ancestral Himalayan river carbonates appear to support this view (Quade et al 1997). Either uplift and/or changing rock distribution on the continents (e.g. Bluth & Kump 1994) could have a major impact on the mean Sr isotopic composition of rivers. For example, the overall trend toward a more radiogenic Sr isotope composition for seawater over the past 150 m.y. or so may be the result not only of decreasing rates of ocean crust formation, but also of the effect of decreasing exposure of young andesitic or basaltic volcanics on the continents—irrespective of global weathering rates.

Another aspect of the Sr isotope problem relates to the residence time of Sr in the ocean. The residence time at present is estimated at 5 m.y. This means that the response of the seawater Sr concentration and isotope ratio to changing inputs is relatively slow; there is little detectable variation at the scale of glacial to interglacial cycles ( $10^5$  yrs.) despite the likelihood that there were significant changes in weathering (e.g. Froelich et al 1992). However, Stoll & Schrag (1996) have argued that the residence time of Sr during the Cretaceous and other times of high sea level may have been considerably shorter (e.g. 1 m.y.) because of the possible extraction of Sr into vast tracts of aragonitic shallow-water carbonates. A relatively short residence time would cause the Sr isotope value of seawater to become more responsive, and therefore possibly appear to be responding to a rapid change in weathering inputs when that is not the case. Thus, the many variables in the Sr isotopic mass balance are difficult to constrain, and render speculation regarding weathering rates in the geologic past rather inconclusive.

Because of neodymium's very short residence time in seawater (on the scale of oceanic mixing times or less, e.g.  $10^2$  yrs), neodymium isotopes are not a panacea for the problems inherent with strontium. However, neodymium does have the unique potential to allow recognition of regional differences in rock types undergoing weathering (e.g. Bertrane & Elderfield 1993). Resolution of trends and changes in Nd isotopes through geologic time will require considerable



effort, in order to resolve intrabasinal versus interbasinal events. The osmium isotope ratio also holds promise—not necessarily as a recorder of global weathering signals, but particularly as an indicator of weathering of Re-rich black shales (Ravizza 1993). As always, the best approach to understanding variations in weathering rate would be to use multiple isotopic proxies.

Ge/Si ratios in biosiliceous sediments hold promise for studies of weathering intensity (e.g. Froelich et al 1992, Shemesh et al 1989). As discussed earlier, the Ge/Si ratio in rivers is much lower than that in hydrothermal fluids. Froelich et al (1992) demonstrated that glacials were characterized by lower Ge/Si in rivers and lower weathering intensity. Because biogenic opal appears to record seawater Ge/Si with fidelity, this proxy is a reasonable monitor of variations in riverine versus hydrothermal sources. As with Sr, however, incongruent dissolution during weathering could lead to changes in the mean riverine Ge/Si representing weathering. In older, diagenetically altered siliceous sediments, the primary Ge/Si ratio may not be preserved; therefore, one must exert care when using this technique.

More general techniques, such as compiling global accumulation rates of carbonate and/or biogenic siliceous deposits, are rife with problems. Oceanic deep-sea carbonate accumulation and the carbonate compensation depth (CCD) are sensitive to changes in accommodation space for carbonate deposition on shelves (e.g. see quantitative treatment by Kump & Arthur 1997). Likewise, the accumulation of biogenic silica, though a probable indicator of silica supply to the oceans, is not a direct indicator of silicate weathering intensity. For example, Froelich et al (1992) suggest that the silica fluxes from rivers were greater by a factor of two during glacials as compared to interglacials, even though the global weathering intensity during glacials was lower on the basis of Ge/Si ratios of seawater.

### Late Ordovician and Late Permian Events: Weathering Inhibited, Climate Warms

There were apparently times in the Phanerozoic when silicate weathering became inefficient as a carbon sink, and when weathering rate, in general, decreased. The weathering rate decrease then had climatic consequences. For example, Gibbs et al (1997) and Kump et al (1999) suggested that the glaciation that took place at the end of the Late Ordovician (Hirnantian) was initiated by  $p\text{CO}_2$  draw-down, which was caused by increased silicate weathering rates associated with increased weatherability of silicate rocks exposed during the Taconic orogeny. Note that this is similar to events proposed for the onset of Neogene glaciation (see below). In this case, glaciation occurred at relatively high  $p\text{CO}_2$  ( $\sim 10\text{XPAL}$ ) compared to present levels, because of the lower solar constant and other factors (Crowley & Baum 1995, Gibbs et al 1997). The glaciation, which lasted perhaps a million years (Marshall et al 1997), was terminated by global warming. Kump et al (1999) suggest that this warming was possibly induced by the buildup of atmospheric carbon dioxide because the areas of exposure of silicate rocks on the continents

were largely covered by glacial ice. Temperate and low-latitude continents were largely covered by limestone deposited during the previous eustatic highstand. Thus weathering became an ineffective sink because, as discussed earlier, weathering of carbonates has no long-term effect on carbon balance. Interestingly, some evidence exists for glacial episodes in the early Silurian as well (Caputo & Crowell 1985). This may suggest that repeated episodes of enhanced silicate weathering and CO<sub>2</sub> draw-down occurred as the ice sheets retreated and the climate warmed.

The latest Permian presents a different possibility regarding climate-weathering feedback. The assembly of Pangaea, a large supercontinent, produced considerable areas of continental aridity (e.g. Ziegler et al 1997). Although glaciation characterized the earlier Permian, continental ice had disappeared by the latest Permian. Arthur et al (1998) suggest that the widespread aridity caused a substantial decrease in weathering rate (weathering-limited) and a drastic reduction of alkalinity and nutrient supply to the oceans. This probably caused an alkalinity crisis in the ocean, and may have had other significant impacts on ocean-atmosphere chemistry, including a possible reduction in  $pO_2$  in the latest Permian (see also Berner & Canfield 1989). The much-reduced weathering rate, as well as decreased organic carbon burial, probably allowed a long-term buildup of volcanic CO<sub>2</sub>, particularly because of the high rates of outgassing associated with the large Siberian Trap eruptions that occurred in the latest Permian/earliest Triassic (Veevers et al 1992, Renne et al 1995). The net effect of the resulting  $pCO_2$  increase was probably global warming and a more active hydrologic cycle. This, in turn, may have contributed to higher rates of weathering and an amelioration of the oceanic nutrient and alkalinity crisis.

### Late Cenozoic and Late Devonian Events: Weathering Enhanced, Climate Cools

Rates of silicate weathering may have been enhanced in the past as the result of certain processes or events. Two of the more controversial hypotheses regarding enhanced weathering and resulting climatic changes revolve around the effects of large-scale tectonic uplift and the rise of vascular plants. As an example of the first process, we discuss the hypothesis that uplift of the Himalayas-Tibetan Plateau and resulting effects on weathering rate,  $pCO_2$ , and climate brought about late Neogene-Quaternary glaciation (Raymo et al 1988, Ruddiman et al 1997). In the second case, we briefly discuss the rise of vascular plants in the Devonian, which may have caused increased weathering rates and a decrease in  $pCO_2$  (Berner 1998) and ushered in the Carboniferous-Permian glacial episode.

Raymo et al (1988) presented a hypothesis for climate change in the Neogene. They cite evidence from pelagic oceanic sequences that indicate increasing accumulation rate of deep-sea carbonates and episodic but rapid increase in the strontium isotopic value of seawater through the Neogene, both of which provide argument for increased global weathering rates and delivery of alkalinity to the oceans. Raymo argues that uplift of the Himalaya-Tibetan Plateau (HTP) largely

accounts for the increased weathering rate. The increased global weathering rate is presumed to have drawn down  $p\text{CO}_2$  and thereby caused global cooling. There appears to be a correspondence between stepwise glacial events and timing of accelerated uplift.

However, Kump & Arthur (1997) suggest that the increased rates of weathering demanded by the Raymo hypothesis lead to an imbalance in the carbon cycle and depletion of the exogenic carbon dioxide inventory. They demonstrate, through judicious use of a geochemical cycle model, that the global rates of chemical erosion did not have to increase through the Cenozoic in response to uplift of the HTP and growth of the continental ice caps. Instead, they suggest that the apparent increase in pelagic carbonate accumulation rates and associated deepening of the calcite compensation depth (CCD) were a response to eustatic sea-level fall and the attendant loss of accommodation space for carbonate deposition on tropical shelves. The rise in the  $^{87}\text{Sr}/^{86}\text{Sr}$  of the oceans was the result of diminishing chemical erosion rates from non-radiogenic (volcanic) source areas and (perhaps) increasing rates from radiogenic source areas.

Nevertheless, the overall climatic cooling through the Cenozoic was most likely the result of a  $\text{CO}_2$  draw-down caused by increasing chemical erosion rates in the HTP and in areas affected by continental glaciation. Pagani et al (1999) have shown that  $p\text{CO}_2$  was near present levels at the beginning of the Miocene, at least 25 million years ago. Their proxy data for  $p\text{CO}_2$  suggest that the stepwise cooling in the Neogene was not related to a trend of decreasing atmospheric carbon dioxide. Thus, whatever its exact timing, the  $\text{CO}_2$  drawdown was not the result of globally increased rates of silicate weathering. Instead, increased silicate weathering rates in areas directly impacted by uplift and glaciation led to slight imbalances in the carbon cycle that were quickly offset by reductions in weathering rates elsewhere. The draw-down in  $p\text{CO}_2$  was regulated by the sensitivity to climate change of weathering in the non-impacted regions. Accelerated uplift and erosion of the HTP would lead to a short-term decline in atmospheric  $p\text{CO}_2$ , but the attendant change in climate would almost instantaneously diminish weathering rates elsewhere, and the carbon cycle would rapidly re-equilibrate. Kump & Arthur (1997) argued that uplift of the HTP decreased the global average soil thickness and residence time, causing a shift in the average erosion regime from more transport-limited to more weathering-limited, to use the terminology of Stallard & Edmond (1983). As discussed earlier, transport-limited regimes are characterized by thick, cation-depleted soils that yield little in the way of a solute load. Chemical erosion rates in these regions are limited by the rate at which the soil mantle is removed from the landscape, and thus tend to be quite slow. Weathering-limited regimes are characterized by thin, immature soils in which there is considerable contact between soil waters and fresh mineral surfaces. Chemical erosion rates in weathering-limited environments are limited only by the rate of mineral dissolution, and thus tend to be quite high. The trend toward weathering limitation would have been furthered by continental glaciation, which

strips the land surface of soil cover and exposes fresh mineral surfaces to weathering attack.

It could be argued that the rise of vascular plants caused a substantial decrease in the equilibrium of  $p\text{CO}_2$ . This would occur because the effect of root development would be to allow more effective penetration of water into soils as well as to supply organic acids, chelates, and carbon dioxide to deeper levels of the soil horizon—all of which would increase weatherability (e.g. Volk 1987). Various workers have suggested that the rise of vascular land plants led to a reduction in  $p\text{CO}_2$  as a result of both increased weathering rate and burial of more refractory carbon (e.g. Robinson 1990, Algeo et al 1995, Retallack 1997, Berner 1998). Berner's (1998) reasoning and quantitative model suggests that weatherability was enhanced about seven-fold while  $p\text{CO}_2$  dropped precipitously from about 12XPAL to 5XPAL as a result of the spread of vascular plants to upland areas. However, there remains some question regarding the relative roles of weathering rate and carbon burial in reducing  $p\text{CO}_2$ . Schwartzman & Volk (1989) argued that lichens and algae, which may have occupied much of the land surface prior to the rise of vascular plants, may have been effective agents of weathering primarily through production of organic acids and chelates. Undoubtedly, the  $p\text{CO}_2$  in equilibrium with an unvegetated land surface would have to be high in relation to that in a largely vegetated world. Berner (1998), however, argues that the surface area covered by lichens and algae is significantly smaller than that effectively interfaced with roots of vascular plants and plant litter. He therefore argues that vascular plants have a greater effect on weathering rate, an idea that appears to be supported by comparative studies of modern vegetated and unvegetated environments (see earlier discussion in this article). Nonetheless, vascular plants also reduce rates of soil erosion more effectively than lichens and algae, so the rise of vascular plants in the late Devonian may have led to thicker soil horizons and more widespread transport-limited settings. Although it is clear that global cooling occurred during and after the Late Devonian, it remains to be demonstrated whether this was primarily due to reduction in  $p\text{CO}_2$  by more effective weathering or to increased rates of organic matter burial. In Berner's GEOCARB modeling, both factors are responsible for the drop in atmospheric  $p\text{CO}_2$  (Figure 10). Inversion of the carbon isotope record requires a large increase in organic carbon burial, which Berner & Canfield (1989) ascribe to the establishment of terrestrial vegetation and coals. In GEOCARB there is a simultaneous increase in the biological weatherability factor, together with a decrease in the calculated silicate weathering rate. A point that is often not well appreciated is that the increase in biological enhancement of weathering did not lead to an increase in the silicate weathering rate; in fact, silicate weathering rates in GEOCARB decreased. If no other change had occurred at 350 Ma, the silicate weathering rate would not have changed—it would have been set by the required balance between volcanic/metamorphic outgassing and imbalances in the organic carbon cycle. As the biological enhancement factor increased, atmospheric  $p\text{CO}_2$  would have decreased, thus decreasing the climatic enhancement of chemical erosion, but not affecting the weathering

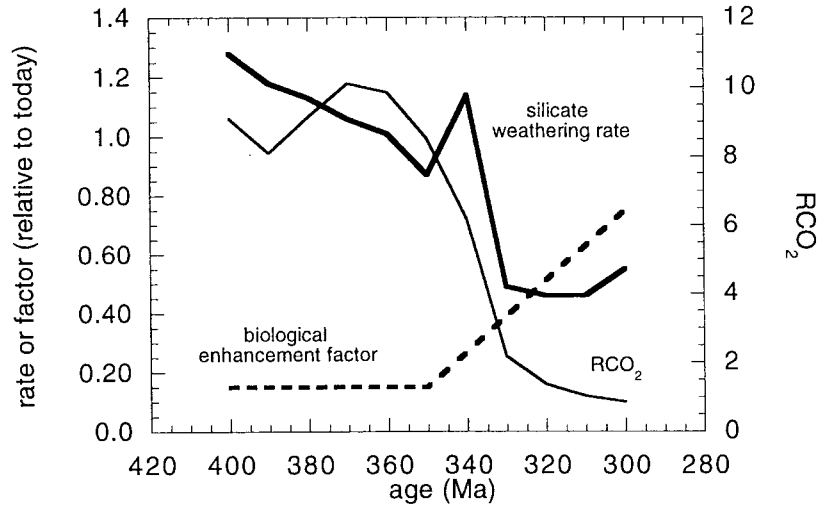


**Figure 10** Silicate weathering rates, biological enhancement factors, and atmospheric  $p\text{CO}_2$  (all relative to today) from the GEOCARB standard model of Berner (1991).

rate. For the interval 400 Ma–350 Ma in GEOCARB, weathering rates generally decreased in response to decreasing outgassing rates and increasing organic carbon burial rates.

One should think of biological enhancement in the same way as one thinks of uplift in terms of chemical erosion: they increase weatherability, but not long-term weathering rates. On the short term, excursions in weathering rate are certainly possible; one should note that there is a brief burst of weathering associated with the upturn in biological enhancement at 350 Ma, which is compensated for by an atmospheric  $p\text{CO}_2$  reduction within the time resolution of the model (in this case, 10 m.y.).

### Precambrian Solar Flux Compensation and Climate Stability

Weathering rate changes that resulted from changing continental exposure in the early Precambrian may have provided a necessary feedback to maintain climate stability in the face of a 30% lower solar flux. Very high  $\text{CO}_2$  outgassing rates for the Archean (Zhang & Zindler 1993) would have produced a high Archean  $p\text{CO}_2$  (perhaps 1–10 bars) that offset the much lower solar flux to the Earth at that time and produced rather warm surface temperatures (e.g. Kasting 1993). However, evidence for glaciations at about 2.5–2.3 Ga and again at about 0.8–0.6 Ga probably required substantially lowered  $p\text{CO}_2$  consistent with much-reduced  $\text{CO}_2$  outgassing and higher rates of carbon recycling to the mantle (Figure 11) for that interval of time. Although the history of continental accretion and

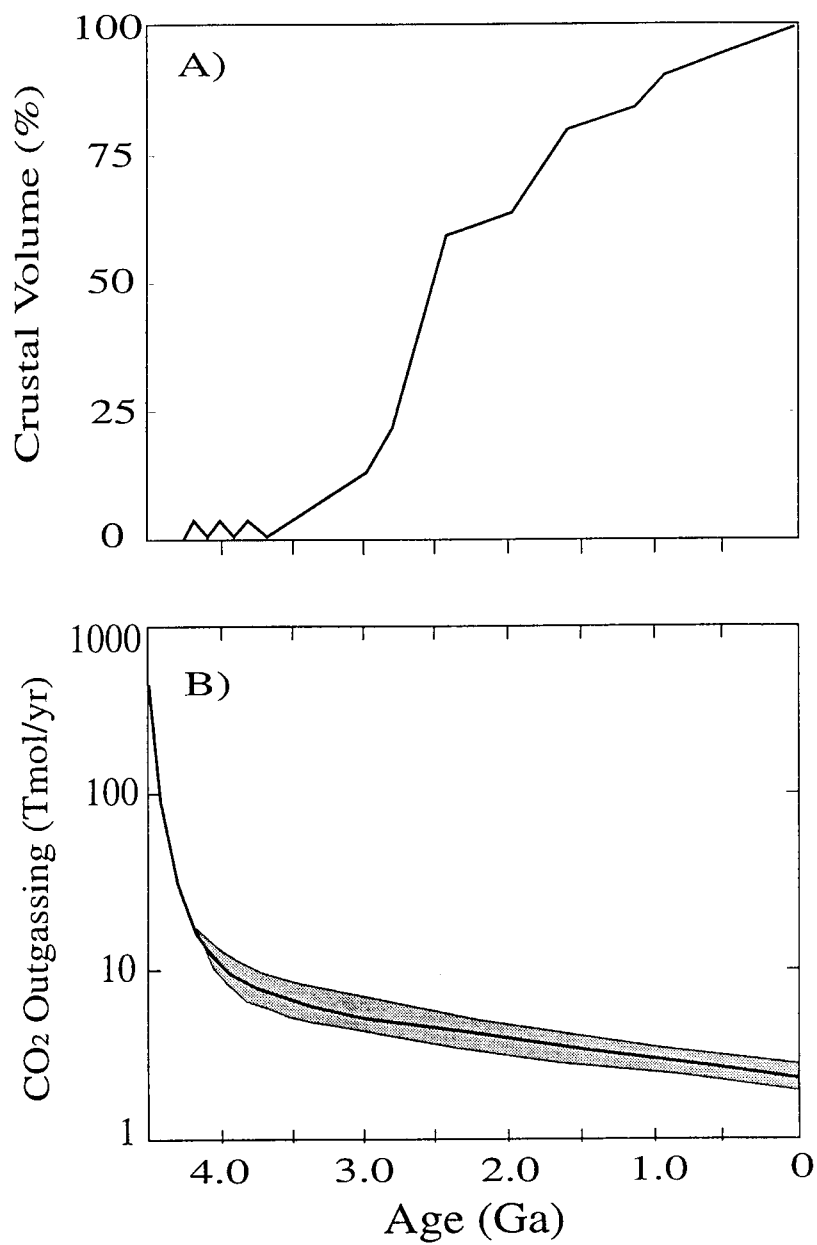


**Figure 11** (A) A suggested crustal growth curve (crustal mass) after Taylor & McLennan (1995); (B) a model for carbon dioxide outgassing rate for the past 4.5 Ga (modified from Zhang & Zindler 1993).

evolution of exposed continental area is still hotly debated (e.g. Bowring & Housh 1995, Taylor & McLennan 1995), most workers agree that the continental mass was not in place until about 2.7 Ga. The Archean/Proterozoic boundary (~2.5 Ga) is thus associated with rapid continental growth, which should have resulted in a large increase in the alkalinity flux to the oceans and the beginnings of carbonate burial in the oceans, as the result of increased continental, silicate weathering rates. Both high  $p\text{CO}_2$  and increasing continental freeboard probably contributed to weathering rate increases. It is not clear when the land surface became colonized by microorganisms on a widespread basis, but it is obvious that weathering in the Precambrian could not have been effective without sufficient exposure of silicate rocks. Thus, the climate history of the period before 2 Ga is consistent with high  $p\text{CO}_2$  sustained by low areas of exposure of continental silicates prior to the Archean/Proterozoic transition, followed by a draw-down in  $p\text{CO}_2$  resulting from a ramp-up of continental silicate weathering associated with a period of rapid continental growth. This allowed the growth of carbonate platforms (Grotzinger 1989) and ultimately led to global glaciation.

## SUMMARY

This paper has addressed the question of the efficacy of the climate-weathering feedback from a number of perspectives. Laboratory studies have contributed fundamental constraints on the mechanism and kinetics of mineral dissolution. Field studies have focused on the controls of river chemistry, and whether they include climate as a major determinant. Numerical modeling is progressing from globally averaged box models to spatially distributed models that can better address the complicated interdependencies that ultimately determine the climatic response of chemical weathering. Also, the geologic record documents a close coupling between climate and weathering throughout the history of Earth.

Laboratory studies of silicate mineral dissolution are now generating high-quality kinetic data that allow for meaningful comparison between laboratory and field determinations of rates of silicate weathering. Such comparisons show, for example, that the relative rates of dissolution of the various silicate minerals are the same in the laboratory and in the field. However, overall rates can differ by orders of magnitudes, and field rates are generally much lower than laboratory rates. An important factor appears to be the flushing rate of soil porewaters, which, when slow, causes solution chemistry to approach equilibrium with some primary or secondary phases and thus retards mineral dissolution rates. Stream data for the various ions indicate that the runoff threshold is near 1 cm/year, above which dilution, rather than chemical equilibrium, becomes an important determinant of stream chemistry. Other factors include temperature, for which well-constrained activation energies have been obtained in the laboratory but only poorly constrained values have been obtained in the field; solution chemistry, including the

effects of organic and carbonic acid concentration; reactive surface area; and biological activity, the effects of which have not been well quantified.

Much of the controversy concerning the climate-weathering feedback has focused on interpretations of river chemical and hydrological data, and whether they reflect chemical erosion sensitivity to climate. Ge/Si ratios indicate that chemical erosion, on a global average, is limited by the rate of supply of dissolved materials during chemical weathering, rather than by the rate of removal of soil mantle. Chemical erosion rates, in turn, seem to be strongly dependent on the intensity of the hydrological cycle, although evidence for temperature dependence seems to be lurking within the convoluted response of chemical erosion rates to climatic differences.

Numerical models highlight the importance of feedback in the carbon cycle to prevent excessive fluctuation in atmospheric  $p\text{CO}_2$  and climate, and the most likely source of feedback is the climate sensitivity of chemical weathering and erosion, which is linked to atmospheric  $p\text{CO}_2$  via the greenhouse effect. However, none of these models has included the role of reverse-weathering processes—though the calculations of McCauley & DePaolo (1997) suggest that future modeling efforts should include reverse weathering.

The geologic record shows not only that climate change has influenced chemical weathering and erosion, but that changes in chemical weathering and erosion have affected climate. Factors such as continental growth and configuration (continentality), tectonic uplift, biological innovation, and solar luminosity have conspired in the past to cause substantial changes in the weatherability of the continents, leading to climate fluctuations, (including the Cenozoic, Ordovician, and Precambrian glaciations), the warmth of intervals such as the Cretaceous, the cooling trend of the late Paleozoic, and the aridity of the Permo-Triassic. Nevertheless, the planet has remained well within the habitability limits of higher organisms for at least the last few billion years, which suggests the presence of a strong regulatory feedback mechanism much like the climate-weathering feedback.

## ACKNOWLEDGMENTS

The authors acknowledge support from the NASA Astrobiology Institute. LRK acknowledges support from the Geology and Paleontology Program at NSF and the EOS MTPE program at NASA. SLB acknowledges DOE Grant No. DE-FG02-95ER14547.A000 and discussions with Yang Chen, whose work comprises much of the analysis summarized in Figures 3, 4, and 7 (Chen 1997). Chen graciously encouraged publication of his work in this format.

**Visit the Annual Reviews home page at [www.AnnualReviews.org](http://www.AnnualReviews.org).**



## LITERATURE CITED

- Alekseyev VA, Medvedeva LS, Prisyagina NI, Meshalkin SS, Balabin AI. 1997. Change in the dissolution rates of alkali feldspars as a result of secondary mineral precipitation and approach to equilibrium. *Geochim. Cosmochim. Acta* 61:1125–42
- Algeo TJ, Berner RA, Maynard JB, Scheckler SE. 1995. Late Devonian oceanic anoxic events and biotic crises: rooted in the evolution of vascular plants? *GSA Today* 5:64–66
- Amiotte-Suchet P, Probst JL. 1993. Modelling of atmospheric CO<sub>2</sub> consumption by chemical weathering of rocks: application to the Garonne, Congo and Amazon basins. *Chem. Geol.* 107:205–10
- Amundson RG, Davidson EA. 1990. Carbon dioxide and nitrogenous gases in the soil atmosphere. *J. Geochem. Explor.* 38:13–41
- Anbeek C. 1992. The dependence of dissolution rates on grain size for some fresh and weathered feldspars. *Geochim. Cosmochim. Acta* 56:3957–70
- Anbeek C. 1993. The effect of natural weathering on dissolution rates. *Geochim. Cosmochim. Acta* 57:4963–75
- Aristovskaya TV, Kutuzova RS. 1968. Microbiological factors in the extraction of silicon from slightly-soluble natural compounds. *Sov. Soil Sci.* 12:1653–59
- Arthur MA. 2000. Volcanic contributions to the carbon and sulfur geochemical cycles and global change. In *Encyclopedia of Volcanoes*, ed. H Sigurdsson, BF Houghton, pp. 1045–56. San Diego: Academic
- Arthur MA, Kump LR, Najjar RG, Hotinski RM, Bice KL. 1998. When the rivers ran dry: an hypothesis for end-Permian mass extinctions. *EOS Trans. Am. Geophys. Union* 79:F405
- Banfield JF, Ferruzzi GG, Casey WH, Westrich HR. 1995. HRTEM study of comparing naturally and experimentally weathered pyroxenoids. *Geochim. Cosmochim. Acta* 59:19–31
- Barker WW, Welch SA, Banfield JF. 1997. Biogeochemical weathering of silicate minerals. In *Geomicrobiology: Interactions Between Microbes and Minerals*, ed. JF Banfield, KH Nealson, 35:391–428. Washington, DC: Mineralogical Soc. Am. Rev. Mineral.
- Barman AK, Varadachari C, Ghosh K. 1992. Weathering of silicate minerals by organic acids. I. Nature of cation solubilisation. *Geoderma* 53:45–63
- Berner EK, Berner RA. 1996. *Global Environment: Water, Air, and Geochemical Cycles*. Upper Saddle River, NJ: Prentice Hall. 376 pp.
- Berner RA. 1978. Rate control of mineral dissolution under earth surface conditions. *Am. J. Sci.* 278:1235–52
- Berner RA. 1981. Kinetics of weathering and diagenesis. *Rev. Miner.* 8:111–34
- Berner RA. 1991. A model for atmospheric CO<sub>2</sub> over Phanerozoic time. *Am. J. Sci.* 291:339–76
- Berner RA. 1994. GEOCARB II: a revised model of atmospheric CO<sub>2</sub> over Phanerozoic time. *Am. J. Sci.* 294:56–91
- Berner RA. 1998. The carbon cycle and CO<sub>2</sub> over Phanerozoic time: the role of land plants. *Philos. Trans. R. Soc. London Ser. B* 53:75–82
- Berner RA, Berner EK. 1997. Silicate weathering and climate. In *Tectonics, Uplift and Climate Change*, ed. W Ruddiman, pp. 353–65. New York: Plenum Publishing Co.
- Berner RA, Caldeira K. 1997. The need for mass balance and feedback in the geochemical carbon cycle. *Geology* 25:955–56
- Berner RA, Canfield DE. 1989. A new model for atmospheric oxygen over Phanerozoic time. *Am. J. Sci.* 289:333–61
- Berner RA, Lasaga AC, Garrels RM. 1983.

- The carbonate-silicate geochemical cycle and its effect on atmospheric carbon dioxide over the past 100 million years. *Am. J. Sci.* 283:641–83
- Berner RA, Rao J-L, Chang S, O'Brien R, Keller CK. 1998. Seasonal variability of adsorption and exchange equilibria in soil waters. *Aquatic Geochem.* 4:273–90
- Bertrane I, Elderfield H. 1993. The geochemical balance of the rare earth elements and Neodymium isotopes in the oceans. *Geochim. Cosmochim. Acta* 57:1957–86
- Blum AE, Lasaga AC. 1988. Role of surface speciation in the low-temperature dissolution of minerals. *Nature* 331:431–33
- Blum AE, Stillings LL. 1995. Feldspar dissolution kinetics. *Rev. Miner.* 31:291–351
- Bluth GJS. 1990. *Effects of paleogeology, chemical weathering, and climate on the global geochemical cycle of carbon dioxide*. PhD thesis. Penn. State Univ., University Park. 130 pp.
- Bluth GJS, Kump LR. 1991. Phanerozoic paleogeology. *Am. J. Sci.* 291:284–308
- Bluth GJS, Kump LR. 1994. Lithologic and climatologic controls of river chemistry. *Geochim. Cosmochim. Acta* 58:2341–59
- Boeglin J-L, Probst J-L. 1998. Physical and chemical weathering rates and CO<sub>2</sub> consumption in a tropical lateritic environment: the upper Niger Basin. *Chem. Geol.* 148:137–56
- Bosecker K. 1993. Bioleaching of silicate manganese ores. *Geomicrob. J.* 11:195–203
- Bowring SA, Housh T. 1995. The Earth's early evolution. *Science* 269:1535–40
- Brady PV, Carroll SA. 1994. Direct effects of CO<sub>2</sub> and temperature on silicate weathering: possible implications for climate control. *Geochim. Cosmochim. Acta* 58:1853–56
- Brady PV, Walther JV. 1992. Surface chemistry and silicate dissolution at elevated temperatures. *Am. J. Sci.* 292:639–58
- Brantley SL, Chen Y. 1995. Chemical weathering rates of pyroxenes and amphiboles. In *Chemical Weathering Rates of Silicate Minerals*, ed. AF White, SL Brantley. *Rev. Miner.* 31:119–72
- Brantley SL, Mellott N. 2000. Surface area and porosity of primary silicate minerals. *Am. Mineral.* Submitted
- Brantley SL, White AF, Hodson ME. 1999. Surface area of primary silicate minerals. In *Growth and Pattern Formation Dissolution in Geosystems*, ed. B Jamtveit, P Meakin, pp. 291–326. Dordrecht, Holland: Kluwer Acad.
- Brunauer S, Emmett PH, Teller E. 1938. Adsorption of gases in multimolecular layers. *J. Am. Chem. Soc.* 60:309–19
- Bruno J, Stumm W, Wersin P, Brandberg F. 1992. On the influence of carbonate in mineral dissolution: I. The thermodynamics and kinetics of hematite dissolution in bicarbonate solutions at T = 25°C. *Geochim. Cosmochim. Acta* 56:1139–47
- Burch TE, Nagy KL, Lasaga AC. 1993. Free energy dependence of albite dissolution kinetics at 80 degrees C and pH 8.8. *Chem. Geol.* 105:137–62
- Caldeira K, Kasting JF. 1992. Susceptibility of the early Earth to irreversible glaciation caused by carbon dioxide clouds. *Nature* 359:226–28
- Caputo MV, Crowell JC. 1985. Migration of glacial centers across Gondwana during the Paleozoic era. *Geol. Soc. Am. Bull.* 97:1026–36
- Carroll-Webb SA, Walther JV. 1990. Kaolinite dissolution at 25°, 60°, and 80°C. *Am. J. Sci.* 290:797–810
- Casey WH, Hochella MF Jr, Westrich HR. 1993. The surface chemistry of manganese silicate minerals as inferred from experiments on tephroite (Mn<sub>2</sub>SiO<sub>4</sub>). *Geochim. Cosmochim. Acta* 57:785–93
- Casey WH, Sposito G. 1992. On the temperature dependence of mineral dissolution rates. *Geochim. Cosmochim. Acta* 56:3825–30
- Chen Y. 1997. *Temperature- and pH-dependence of silicate dissolution rate at acid pH*. PhD thesis. Penn. State Univ., University Park. 220 pp.
- Chen Y, Brantley SL. 1997. Temperature- and

- pH-dependence of albite dissolution rate at acid pH. *Chem. Geol.* 135:275–92
- Chen Y, Brantley SL. 1998. Diopside and anthophyllite dissolution at 25°C and 90°C and acid pH. *Chem. Geol.* 147:233–48
- Chen Y, Brantley SL. 2000. Dissolution of forsteritic olivine at 65°C and  $2 < \text{pH} < 5$ . *Chem. Geol.* In press
- Coston JA, Fuller CC, Davis JA. 1995.  $\text{Pb}^{2+}$  and  $\text{Zn}^{2+}$  adsorption by a natural aluminum- and iron-bearing surface coating on an aquifer sand. *Geochim. Cosmochim. Acta* 59:3535–47
- Crowley TJ, Baum SK. 1995. Reconciling late Ordovician (440 Ma) glaciation with very high (14x)  $\text{CO}_2$  levels. *J. Geophys. Res.* 100:1093–101
- Cygan RT, Casey WH, Roslough MB, Westrich HR, Carr MJ, Holdren GR. 1989. Dissolution kinetics of experimentally shocked silicate minerals. *Chem. Geol.* 78:229–44
- Dahlgren RA, Boettinger JL, Huntington GL, Amundson RG. 1997. Soil development along an elevational transect in the western Sierra Nevada, California. *Geoderma* 78:207–36
- Davis JA, Fuller CC, Coston JA, Hess KM, Dixon E. 1993. Spatial heterogeneity of geochemical and hydrologic parameters affecting metal transport in ground water. *EPA Environmental Research Brief, EPA/600/S-93/006*
- Delaney M, Boyle E. 1986. Lithium in foraminiferal shells: implications for high-temperature hydrothermal fluxes and oceanic crustal generation rates. *Earth Planet. Sci. Lett.* 80:91–105
- Delaney ML, Filippelli GM. 1994. An apparent contradiction in the role of phosphorus in Cenozoic chemical mass balances for the world ocean. *Paleoceanography* 9:513–27
- Denison RE, Koepnick RB, Burke WH, Hetherington EA. 1998. Construction of the Cambrian and Ordovician seawater  $^{87}\text{Sr}/^{86}\text{Sr}$  curve. *Chem. Geol.* 152:325–40
- Dorn RI, Brady PV. 1995. Rock based measurement of temperature dependent plagioclase weathering. *Geochim. Cosmochim. Acta* 59:2847–52
- Drever JI. 1988. *The Geochemistry of Natural Waters*. Upper Saddle River, NJ: Prentice Hall. 437 pp. 2nd ed.
- Drever JI. 1994. The effect of landplants on weathering rates of silicate minerals. *Geochim. Cosmochim. Acta* 58:2325–33
- Drever JI, Zobrist J. 1992. Chemical weathering of silicate rocks as a function of elevation in the southern Swiss Alps. *Geochim. Cosmochim. Acta* 56:3209–216
- Duff RB, Webley DM, Scott RO. 1963. Solubilization of minerals and related materials by 2-ketogluconic acid-producing bacteria. *Soil Sci.* 95:105–14
- Edmond JM. 1992. Himalayan tectonics, weathering processes, and the strontium isotope record in marine limestones. *Science* 258:1594–97
- Edmond JM, Huh Y. 1997. Chemical weathering yields from basement and orogenic terrains in hot and cold climates. In *Tectonics, Uplift and Climate Change*, ed. W Rudiman, pp. 329–51. New York: Plenum Publishing Co.
- Edmond JM, Palmer MR, Measures CI, Grant B, Stallard RF. 1995. The fluvial geochemistry and denudation rate of the Guayana Shield in Venezuela, Colombia, and Brazil. *Geochim. Cosmochim. Acta* 59:3301–25
- Eggleston CM, Hochella MF Jr, Parks GA. 1989. Sample preparation and aging on the dissolution rate and surface composition of diopside. *Geochim. Cosmochim. Acta* 53:797–804
- Ferruzzi GG. 1993. *The character and rates of dissolution of pyroxenes and pyroxenoids*. MS thesis, University of California, Davis. 105 pp.
- Fischer AG. 1982. Long-term climatic oscillations recorded in stratigraphy. In *Climate in Earth History*, pp. 97–104. Washington, DC: National Academy of Sciences.
- Follmi KB. 1995. 160 m.y. record of marine sedimentary phosphorus burial: coupling of climate and continental weathering under

- greenhouse and icehouse conditions. *Geology* 23:859–62
- Frakes LA, Francis JE, Syktus JI. 1992. *Climate Modes of the Phanerozoic: The History of the Earth's Climate over the Past 600 Million Years*. New York: Cambridge. 274 pp.
- France-Lanord C, Derry LA. 1997. Organic carbon burial forcing of the carbon cycle from Himalayan erosion. *Nature* 390:65–67
- Froelich PN, Blanc V, Mortlock RA, Chillrud SN, Dunstan W, et al. 1992. River fluxes of dissolved silica to the ocean were higher during glacial: Ge/Si in diatoms, rivers, and oceans. *Paleoceanography* 7:739–67
- Froelich PN, Hambrick GA, Andreae MO, Mortlock RA, Edmond JM. 1985. The geochemistry of inorganic germanium in natural waters. *J. Geophys. Res.* 90:1133–41
- Gaillardet J, Dupre B, Allegre CJ. 1995. A global geochemical mass budget applied to the Congo Basin rivers: erosion rates and continental crust composition. *Geochim. Cosmochim. Acta* 59:3469–85
- Garrels RM, Mackenzie FT. 1967. Origin of the chemical compositions of some springs and lakes. In *Equilibrium Concepts in Natural Water Systems*, ed. RF Gould, pp. 222–42. Washington, DC: American Chemical Society
- Garrels RM, Mackenzie FT, Hunt C. 1975. *Chemical Cycles and the Global Environment: Assessing Human Influences*. Los Altos, CA: William Kaufmann, Inc. 206 pp.
- Gautier J-M, Oelkers EH, Schott J. 1994. Experimental study of K-feldspar dissolution rates as a function of chemical affinity at 150°C and pH 9. *Geochim. Cosmochim. Acta* 58:68–88
- Gibbs MT, Barron EJ, Kump LR. 1997. An apparent pCO<sub>2</sub> threshold for glaciation in the Late Ordovician. *Geology* 25:447–50
- Gibbs MT, Bluth GS, Fawcett PJ, Kump LR. 1999. Chemical weathering over the last 240 Myr: variations due to changes in paleogeography, paleoclimate, and paleogeology. *Am. J. Sci.* 299:611–51
- Gibbs MT, Kump LR. 1994. Global chemical erosion at the last glacial maximum and the present: sensitivity to changes in lithology and hydrology. *Paleoceanography* 9:529–43
- Gibbs RJ. 1970. Mechanisms controlling world water chemistry. *Science* 170:1088–90
- Gislason SR, Arnorsson S. 1993. Dissolution of primary basaltic minerals in natural waters: saturation state and kinetics. *Chem. Geol.* 105:117–35
- Gislason SR, Arnorsson S, Armannsson H. 1996. Chemical weathering of basalt in southwest Iceland: effects of runoff, age of rocks and vegetative/glacial cover. *Am. J. Sci.* 296:837–907
- Grandstaff DE. 1977. Some kinetics of bron-zite orthopyroxene dissolution. *Geochim. Cosmochim. Acta* 41:1097–103
- Grandstaff DE. 1980. The dissolution of forsteritic olivine from Hawaiian beach sand. *Proc. 3rd Int. Symp. Water-Rock Interaction*, pp. 72–74
- Grandstaff DE. 1986. The dissolution rate of forsteritic olivine from Hawaiian beach sand. In *Rates of Chemical Weathering of Rocks and Minerals*, ed. SM Colman, DP Dethier, pp. 41–57. Orlando, FL: Academic Press
- Gregg SJ, Sing KSW. 1982. *Adsorption, Surface Area and Porosity*. London: Academic Press. 303 pp.
- Grotzinger JP. 1989. Facies and evolution of Precambrian carbonate depositional systems: emergence of the modern platform archetype. In *Controls on Carbonate Platform and Basin Development*, ed. PD Crevello, pp. 79–106. Tulsa, OK: Soc. Econ. Paleontol. Mineral. Spec. Publ. 44. 405 pp.
- Gwiazda RH, Broecker WS. 1994. The separate and combined effects of temperature, soil pCO<sub>2</sub>, and organic acidity on silicate weathering in the soil environment: formulation of a model and results. *Global Biogeochem. Cycles* 8:141–55
- Heaney PJ, Post JE. 1992. The widespread distribution of a novel silica polymorph in microcrystalline quartz varieties. *Science* 255:441–43

- Helgeson HC, Murphy WM, Aagard P. 1984. Thermodynamic and kinetic constraints on reaction rates among minerals and aqueous solutions II. Rate constants, effective surface area, and the hydrolysis of feldspar. *Geochim. Cosmochim. Acta* 48:2405–32
- Hellmann R. 1994. The albite-water system: Part I. The kinetics of dissolution as a function of pH at 100, 200, and 300°C. *Geochim. Cosmochim. Acta* 58:595–611
- Hewkin DJ, Prince RH. 1970. The mechanism of octahedral complex formation by labile metal ions. *Coord. Chem. Rev.* 5:45–73
- Hochella MF, Banfield J. 1995. Chemical weathering of silicates in nature: a microscopic perspective with theoretical considerations. *Rev. Miner.* 31:353–406
- Hodson ME. 1999. Micropore surface area variation with grain size in unweathered alkali feldspars—implications for surface roughness and dissolution studies. *Geochim. Cosmochim. Acta* 63:3429–35
- Holland HD. 1978. *The Chemistry of the Atmosphere and Oceans*. New York: Wiley-Interscience. 351 pp.
- Huh Y, Edmond JM. 1999. The fluvial geochemistry of the rivers of eastern Siberia: III, Tributaries of the Lena and Anabar draining the basement terrain of the Siberian Craton and the Trans-Baikal Highlands. *Geochim. Cosmochim. Acta* 63:967–87
- Ivarson KC, Ross GJ, Miles NM. 1978. Alterations of micas and feldspars during microbial formation of basic ferric sulfates in the laboratory. *Soil Sci. Soc. Am. J.* 42:518–24
- Ivarson KC, Ross GJ, Miles NM. 1979. The microbiological formation of basic ferric sulfates. II. Crystallization in presence of potassium-, ammonium-, and sodium-salts. *Soil Sci. Soc. Am. Proc.* 43:908–12
- Ivarson KC, Ross GJ, Miles NM. 1980. The microbiological formation of basic ferric sulfates. 3. Influence of clay minerals on crystallization. *Can. J. Soil Sci.* 60:137–40
- Kasting JF. 1993. Earth's early atmosphere. *Science* 259:920–26
- Keil H, Schwartz W. 1980. Leaching of a silicate and carbonate copper ore with heterotrophic fungi and bacteria, producing organic acids. *Z. Allg. Mikrobiol.* 20:627–36
- Knauss KG, Nguyen SN, Weed HC. 1993. Diopside dissolution kinetics as a function of pH, CO<sub>2</sub>, temperature, and time. *Geochim. Cosmochim. Acta* 57:285–94
- Krauskopf KB. 1979. Introduction to geochemistry. In *International Series in the Earth and Planetary Sciences*, ed. KB Krauskopf, KO Emery, RF Legget, B Murray, LL Sloss, 617 pp. New York: McGraw-Hill. 2nd ed.
- Kump LR. 1996. The physiology of the planet. *Nature* 381:111–12
- Kump LR, Arthur MA. 1997. Global chemical erosion during the Cenozoic: weatherability balances the budget. In *Tectonics, Uplift and Climate Change*, ed. W Ruddiman, pp. 399–426. New York: Plenum Publishing Co.
- Kump LR, Arthur MA, Patzkowsky ME, Gibbs MT. 1999. A weathering hypothesis for glaciation at high atmospheric pCO<sub>2</sub> during the Late Ordovician. *Palaeogeog. Palaeoclim. Palaeoecol.* 152:173–87
- Kump LR, Kasting JF, Crane RG. 1999. *The Earth System*. Upper Saddle River, NJ: Prentice Hall. 351 pp.
- Kump LR, Volk T. 1991. Gaia's garden and BLAG's greenhouse: global biogeochemical climate regulation. In *Scientists on Gaia*, ed. SH Schneider, PJ Boston, pp. 191–99. Boston: MIT Press
- Kutuzova RS. 1973. Possible ways of mineral weathering in alkaline soils. *Sov. Soil Sci.* 1:111–16
- Laidler K. 1987. *Chemical Kinetics*. New York: Harper & Row. 531 pp. 3rd ed.
- Lasaga AC, Berner RA, Garrels RM. 1985. An improved geochemical model of atmospheric carbon dioxide. In *The Carbon Cycle and Atmospheric CO<sub>2</sub>: Natural Variations Archean to Present*, ed. ET Sundquist, WS Broecker. *Am. Geophys. Union Geophys. Monogr.* 32:397–411
- Lasaga AC, Soler JM, Ganor J, Burch TE, Nagy KL. 1994. Chemical weathering rate

- laws and global geochemical cycles. *Geochim. Cosmochim. Acta* 58:2361–86
- Lee MR, Hodson ME, Parsons I. 1998. The role of intragranular microtextures and microstructures in chemical and mechanical weathering: direct comparisons of experimentally and naturally weathered alkali feldspars. *Geochim. Cosmochim. Acta* 62:2771–88
- Liermann LJ, Kalinowski BE, Brantley SL, Ferry JG. 2000. Role of bacterial siderophores in dissolution of hornblende. *Geochim. Cosmochim. Acta*. In press
- Luce RW, Bartlett WB, Parks GA. 1972. Dissolution kinetics of magnesium silicates. *Geochim. Cosmochim. Acta* 36:35–50
- Ludwig W, Amiotte-Suchet P, Munhoven G, Probst J-L. 1998. Atmospheric CO<sub>2</sub> consumption by continental erosion: present-day controls and implications for the last glacial maximum. *Global Planet. Change* 16–17:107–20
- Ludwig W, Amiotte-Suchet P, Probst JL. 1996. River discharges of carbon to the world's oceans: determining local inputs of alkalinity and of dissolved and particulate organic carbon. *Acad. Sci. C. R.* 323:1007–14
- Mackenzie FT, Garrels RM. 1966. Chemical mass balance between rivers and oceans. *Am. J. Sci.* 264:507–25
- Mackenzie FT, Kump LR. 1995. Reverse weathering, clay mineral formation, and oceanic element cycles. *Science* 270:586–87
- Malinovskaya IM, Kosenko LV, Votselko SK, Podgorskii VS. 1990. Role of Bacillus mucilaginous polysaccharide in degradation of silicate minerals. *Mikrobiologiya* 59:70–78 (Engl. transl. pp. 49–55)
- Marshall JD, Brenchley PJ, Mason P, Wolff GA, Astini RA, et al. 1997. Global carbon isotopic events associated with mass extinction and glaciation in the late Ordovician. *Palaeogeog. Palaeoclimatol. Palaeoecol.* 132:195–210
- Mast MA, Drever JI. 1987. The effect of oxalate on the dissolution rates of oligoclase and tremolite. *Geochim. Cosmochim. Acta* 51:2559–68
- McCauley SE, DePaolo DJ. 1997. The marine <sup>87</sup>Sr/<sup>86</sup>Sr and δ<sup>18</sup>O records, Himalayan alkalinity fluxes and Cenozoic climate models. In *Tectonics, Uplift and Climate Change*, ed. W Ruddiman, pp. 428–67. New York: Plenum Publishing Co.
- Meybeck M. 1980. Pathways of major elements from land to ocean through rivers. In *Proceedings of the Review and Workshop on River Inputs to Ocean System*, ed. J-M Martin, JD Burton, D Eisma, pp. 18–30. Rome: FAO (Food and Agricultural Organization of the United Nations)
- Michalopoulos P, Aller RC. 1995. Rapid clay mineral formation in Amazon Delta sediments: reverse weathering and oceanic elemental cycles. *Science* 270:614–17
- Miller WR, Drever JI. 1977. Water chemistry of a stream following a storm, Absaroka Mountains, Wyoming. *Geol. Soc. Am. Bull.* 88:286–90
- Mortlock RA, Froelich PN. 1987. Continental weathering of germanium: Ge/Si in the global river discharge. *Geochim. Cosmochim. Acta* 51:2075–82
- Murnane RJ, Stallard RF. 1990. Germanium and silicon in rivers of the Orinoco drainage basin. *Nature* 344:749–52
- Murphy SF, Brantley SL, Blum AE, White AF, Dong H. 1998. Chemical weathering in a tropical watershed, Luquillo Mountains, Puerto Rico: II. Rate and mechanism of biotite weathering. *Geochim. Cosmochim. Acta* 62:227–43
- Murphy WM. 1985. *Thermodynamic and kinetic constraints on reaction rates among minerals and aqueous solutions*. PhD dissertation, University of California, Berkeley. 165 pp.
- Nickel E. 1973. Experimental dissolution of light and heavy minerals in comparison with weathering and intrastatal solution. *Contrib. Sediment.* 1:3–68
- Nugent MA, Brantley SL, Pantano CG, Maurice PA. 1998. The influence of natural mineral coatings on feldspar weathering. *Nature* 395:588–91
- Paces T. 1983. Rate constants of dissolution derived from the measurements of mass

- balance in hydrological catchments. *Geochim. Cosmochim. Acta* 47:1855–63
- Pagani M, Arthur MA, Freeman KH. 1999. Miocene evolution of atmospheric carbon dioxide. *Paleoceanography* 14:273–92
- Probst J-L, Mortatti J, Tardy Y. 1994. Carbon river fluxes and weathering CO<sub>2</sub> consumption in the Congo and Amazon river basins. *Appl. Geochem.* 9:1–13
- Quade J, Roe L, DeCelles P, Ojha TP. 1997. The Late Neogene 87Sr/86Sr record of lowland Himalayan rivers. *Science* 276:1828–31
- Ravizza G. 1993. Variations of the <sup>187/186</sup>Os ratio of seawater over the past 28 million years as inferred from metalliferous carbonates. *Earth Planet. Sci. Lett.* 118:335–48
- Raymo ME. 1997. Carbon cycle models: how strong are the constraints? In *Tectonics, Uplift and Climate Change*, ed. W Ruddiman, pp. 367–81. New York: Plenum Publishing Co.
- Raymo ME, Ruddiman WF, Froelich PN. 1988. Influence of late Cenozoic mountain building on ocean geochemical cycles. *Geology* 16:649–53
- Renne PR, Zhang ZC, Richards MA, Black MT, Basu AR. 1995. Synchrony and causal relations between Permian-Triassic boundary crises and Siberian flood volcanism. *Science* 269:1413–16
- Retallack GJ. 1997. Early forest soils and their role in Devonian global change. *Science* 276:583–85
- Richards PJJ. 1999. *Chemical weathering in watersheds: theoretical and field studies in the Mahantango Creek and Susquehanna River Basins, Pennsylvania*. PhD thesis. Penn. State Univ., University Park. 236 pp.
- Rickard DT. 1973. Sedimentary iron sulphide formation. In *Acid Sulfate Soils*, ed. H Dost, ILRI Publ. 18, Vol. 1, pp. 28–62. Wageningen, The Netherlands: Institute for Land Reclamation and Improvement
- Rimstidt JD, Dove PM. 1986. Mineral/solution reaction rates in a mixed flow reactor: wollastonite hydrolysis. *Geochim. Cosmochim. Acta* 50:2509–16
- Robert M, Berthelin J. 1986. Role of biological and biochemical factors in soil mineral weathering. In *Interactions of Soil Minerals with Natural Organics and Microbes*, ed. PM Huang, M Schnitzer, pp. 453–95. Madison, WI: Soil Science Society of America
- Robinson JM. 1990. The burial of organic carbon as affected by the evolution of land plants. *Hist. Biol.* 3:189–201
- Rosso JJ, Rimstidt JD. 2000. A high resolution study of forsterite dissolution at 1.8 < pH < 3.8 and 25 < °C < 45. *Geochim. Cosmochim. Acta*. In press
- Ruddiman WF. 1997. *Tectonics, Uplift and Climate Change*. New York: Plenum Publishing Co. 535 pp.
- Ruddiman WF, Raymo ME, Prell WL, Kutzbach JE. 1997. The uplift-climate connection: a synthesis. In *Tectonics, Uplift and Climate Change*, ed. W Ruddiman, pp. 471–516. New York: Plenum Publishing Co.
- Russell JD, Paterson E, Fraser AR, Farmer VC. 1975. Adsorption of carbon dioxide on goethite surfaces, and its implications for anion adsorption. *Chem. Soc., Faraday Trans. 1* 71:1623–30
- Sagan C, Mullen G. 1972. Earth and Mars: evolution of atmospheres and surface temperatures. *Science* 177:52–56
- Schnoor JL. 1990. Kinetics of chemical weathering: a comparison of laboratory and field weathering rates. In *Aquatic Chemical Kinetics: Reaction Rates of Processes in Natural Waters*, ed. W Stumm, pp. 475–504. Zurich: Swiss Fed. Inst. Technol.
- Schott J, Berner RA. 1983. X-ray photoelectron studies of the mechanism of iron silicate dissolution during weathering. *Geochim. Cosmochim. Acta* 47:2233–40
- Schott J, Berner RA, Sjöberg EL. 1981. Mechanism of pyroxene and amphibole weathering—I. Experimental studies of iron-free minerals. *Geochim. Cosmochim. Acta* 45:2123–35
- Schwartzman DW, Volk T. 1989. Biotic enhancement of weathering and the habitability of earth. *Nature* 340:457–60

- Shemesh A, Mortlock R, Froelich P. 1989. Late Cenozoic Ge/Si record of marine biogenic opal: implications for variations of riverine fluxes to the ocean. *Paleoceanography* 4:221–34
- Sillen LG. 1961. The physical chemistry of sea water. In *Oceanography—Invited Lectures Presented at the International Oceanography Congress*, ed. M Sears, pp. 549–81. Washington, DC: Am. Assoc. Adv. Sci. Publ. 67
- Sloan LC, Bluth GJS, Filippelli GM. 1997. A comparison of spatially resolved and global mean reconstructions of continental denudation under ice-free and present conditions. *Paleoceanography* 12:147–60
- Stallard RF. 1985. River chemistry, geology, geomorphology, and soils in the Amazon and Orinoco basins. In *The Chemistry of Weathering*, ed. JI Drever, pp. 293–316. Dordrecht, Holland: D. Reidel Publ. Co.
- Stallard RF, Edmond JM. 1981. Geochemistry of the Amazon 1. Precipitation chemistry and the marine contribution to the dissolved load at the time of peak discharge. *J. Geophys. Res.* 86:9844–58
- Stallard RF, Edmond JM. 1983. Geochemistry of the Amazon 2. The influence of geology and weathering environment on the dissolved load. *J. Geophys. Res.* 88:9671–88
- Stallard RF, Edmond JM. 1987. Geochemistry of the Amazon 3. Weathering chemistry and limits to dissolved inputs. *J. Geophys. Res.* 92:8293–302
- Staudigal H, Hart SR, Schmincke H-U, Smith BM. 1989. Cretaceous ocean crust at DSDP sites 417 and 418: carbon uptake from weathering vs. loss by magmatic outgassing. *Geochim. Cosmochim. Acta* 53:3091–94
- Stillings LL, Brantley SL. 1995. Feldspar dissolution at 25°C and pH 3: reaction stoichiometry and the effect of cations. *Geochim. Cosmochim. Acta* 59:1483–96
- Stillings LL, Drever JI, Brantley SL, Sun Y, Oxburgh R. 1996. Rates of feldspar dissolution at pH 3–7 with 0–8 mM oxalic acid. *Chem. Geol.* 132:79–90
- Stoll HM, Schrag DP. 1996. Evidence for glacial control of rapid sea level changes in the Early Cretaceous. *Science* 272:1771–74
- Sverdrup HU. 1990. *The Kinetics of Base Cation Release Due to Chemical Weathering*. Lund, Sweden: Lund Univ. Press. 246 pp.
- Sverjensky DA. 1992. Linear free energy relations for predicting dissolution rates of solids. *Nature* 358:310–13
- Sverjensky DA. 1994. Zero-point-of-charge prediction from crystal chemistry and solvation theory. *Geochim. Cosmochim. Acta* 58:3123–29
- Swoboda-Colberg NG, Drever JI. 1993. Mineral dissolution rates in plot-scale field and laboratory experiments. *Chem. Geol.* 105:51–69
- Tardy Y, N’Koukou R, Probst JL. 1989. The global water cycle and continental erosion during Phanerozoic time (570 my). *Am. J. Sci.* 289:455–83
- Taylor SR, McLennan SM. 1995. The geochemical evolution of the continental crust. *Rev. Geophys.* 33:241–65
- Ullman WJ, Kirchman DL, Welch SA, Vandevivere P. 1996. Laboratory evidence for microbially mediated silicate mineral dissolution in nature. *Chem. Geol.* 132:11–17
- Urrutia MM, Beveridge TJ. 1994. Formation of fine-grained metal and silicate precipitates on a bacterial surface (*Bacillus subtilis*). *Chem. Geol.* 116:261–80
- van der Sluijs JP, de Bruyn GJ, Westbroek P. 1996. Biogenic feedbacks in the carbonate-silicate geochemical cycle and the global climate. *Am. J. Sci.* 296:932–53
- Van Geen A, Robertson AP, Leckie JO. 1994. Complexation of carbonate species at the goethite surface: implications for adsorption of metal ions in natural waters. *Geochim. Cosmochim. Acta* 58:2073–86
- Varekamp JC, Kreulen R, Poorter RPE, Van Bergen MJ. 1992. Carbon sources in arc volcanism: with implications for the carbon cycle. *Terra Nova* 4:363–73
- Veevers JJ, Conaghan PJ, Shaw SE. 1992. Turning point in Pangean environmental history at the Permian/Triassic (P/Tr) boundary. In *Pangea: Paleoclimate, Tecton-*



- ics, and Sedimentation During Accretion, Zenith and Breakup of a Supercontinent*, ed. Klein GD. Geol. Soc. Am. Spec. Pap. 288:187–96
- Velbel MA. 1985. Geochemical mass balances and weathering rates in forested watersheds of the southern Blue Ridge. *Am. J. Sci.* 285:904–30
- Velbel MA. 1989. Effect of chemical affinity on feldspar hydrolysis rates in two natural weathering systems. *Chem. Geol.* 78:245–53
- Velbel MA. 1993. Temperature dependence of silicate weathering in nature: how strong a negative feedback on long-term accumulation of atmospheric CO<sub>2</sub> and global greenhouse warming? *Geology* 21:1057–192
- Volk T. 1987. Feedbacks between weathering and atmospheric CO<sub>2</sub> over the last 100 million years. *Am. J. Sci.* 287:763–79
- Walker JCG, Hays PB, Kasting JF. 1981. A negative feedback mechanism for the long-term stabilization of Earth's surface temperature. *J. Geophys. Res.* 86:9776–82
- Welch SA, Vandevivere P. 1994. Effect of microbial and other naturally occurring polymers on mineral dissolution. *Geomicrobiol. J.* 12:227–38
- Westrich HR, Cygan RT, Casey WH, Zemitis C, Arnold GW. 1993. The dissolution kinetics of mixed-cation orthosilicate minerals. *Am. J. Sci.* 293:869–93
- White AF. 1995. Chemical weathering rates of silicate minerals in soils. *Rev. Miner.* 31:407–62
- White AF, Blum AE. 1995. Effects of climate on chemical weathering in watersheds. *Geochim. Cosmochim. Acta* 59:1729–47
- White AF, Brantley SL. 1995. Chemical weathering rates of silicate minerals: an overview. In *Chemical Weathering Rates of Silicate Minerals*, ed. AF White, SL Brantley. *Rev. Miner.* 31:1–22
- White AF, Peterson ML. 1990. Role of reactive-surface-area characterization in geochemical kinetic models. *Chemical Modeling of Aqueous Systems II. Am. Chem. Soc. Symp. Ser.* 416:461–75
- Wogelius RA, Walther JV. 1991. Olivine dissolution at 25°C: effects of pH, CO<sub>2</sub>, and organic acids. *Geochim. Cosmochim. Acta* 55:943–54
- Wogelius RA, Walther JV. 1992. Olivine dissolution kinetics at near-surface conditions. *Chem. Geol.* 97:101–12
- Worsley TR, Nance RD, Moody JB. 1988. Tectonics, carbon, life, and climate for the last three billion years: a unified system? In *Scientists on Gaia*, ed. SH Schneider, PJ Boston, pp. 200–10. Cambridge, MA: MIT Press.
- Xie Z. 1994. *Surface properties of silicates, their solubility and dissolution kinetics*. PhD thesis. Northwestern Univ., Evanston, IL. 163 pp.
- Yau S. 1999. *Dissolution kinetics of feldspar in the Cape Cod Aquifer, Massachusetts*. MS, Pennsylvania State Univ., University Park. 99 pp.
- Zeltner WA, Anderson MA. 1988. Surface charge development at the goethite/aqueous solution interface: effects of CO<sub>2</sub> adsorption. *Langmuir* 4:469–74
- Zhang Y, Zindler A. 1993. Distribution and evolution of carbon and nitrogen in Earth. *Earth Planet. Sci. Lett.* 117:331–45
- Ziegler AM, Hulver ML, Rowley DB. 1997. Permian world topography and climate. In *Late Glacial and Postglacial Environmental Changes: Quaternary, Carboniferous-Permian, and Proterozoic*, ed. IP Martini, pp. 111–42. New York: Oxford University Press.





## CONTENTS

Palynology after Y2K--Understanding the Source Area of Pollen in Sediments, <i>M. B. Davis</i>	1
Dinosaur Reproduction and Parenting, <i>John R. Horner</i>	19
Evolution and Structure of the Lachlan Fold Belt (Orogen) of Eastern Australia, <i>David A. Foster, David R. Gray</i>	47
Remote Sensing of Active Volcanoes, <i>Peter Francis, David Rothery</i>	81
Dynamics of Volcanic Systems in Iceland: Example of Tectonism and Volcanism at Juxtaposed Hot Spot and Mid-Ocean Ridge Systems, <i>Agust Gudmundsson</i>	107
Understanding Oblique Impacts from Experiments, Observations, and Modeling, <i>E. Pierazzo, H. J. Melosh</i>	141
Synthetic Aperture Radar Interferometry to Measure Earth's Surface Topography and Its Deformation, <i>Roland Bürgmann, Paul A. Rosen, Eric J. Fielding</i>	169
Geologic Evolution of the Himalayan-Tibetan Orogen, <i>An Yin, T. Mark Harrison</i>	211
MARS 2000, <i>Arden L. Albee</i>	281
Vredefort, Sudbury, Chicxulub: Three of a Kind, <i>Richard Grieve, Ann Therriault</i>	305
Climate Reconstruction from Subsurface Temperatures, <i>Henry N. Pollack, Shaopeng Huang</i>	339
Asteroid Fragmentation and Evolution of Asteroids, <i>Eileen V. Ryan</i>	367
Seismic Imaging of Mantle Plumes, <i>Henri-Claude Nataf</i>	391
New Perspectives on Orbitally Forced Stratigraphy, <i>Linda A. Hinnov</i>	419
Clathrate Hydrates, <i>Bruce A. Buffett</i>	477
Heterogeneity of the Lowermost Mantle, <i>Edward J. Garnero</i>	509
Spreading Volcanoes, <i>Andrea Borgia, Paul T. Delaney, Roger P. Denlinger</i>	539
Scaling, Universality, and Geomorphology, <i>Peter Sheridan Dodds, Daniel H. Rothman</i>	571
Chemical Weathering, Atmospheric CO <sub>2</sub> , and Climate, <i>Lee R. Kump, Susan L. Brantley, Michael A. Arthur</i>	611
Self-Ordering and Complexity in Epizonal Mineral Deposits, <i>Richard W. Henley, Byron R. Berger</i>	669